Revised Review Article

Title page

Molecular Mechanisms of PTH/PTHrP class B GPCR Signaling and Pharmacological Implications

Jean-Pierre Vilardaga[1] PhD; Lisa J. Clark[1], PhD; Alex D. White[1], PhD; Ieva Sutkeviciute[1], PhD; Ji Young Lee[2], PhD; Ivet Bahar[2,] PhD.

[1]Laboratory for GPCR Biology, Department of Pharmacology and Chemical Biology, and [2]Department of Computational and Systems Biology, University of Pittsburgh School of Medicine, Pittsburgh PA 15261, USA.

Laboratory for GPCR Biology, Department of Pharmacology and Chemical Biology, and Department of Computational and Systems Biology, University of Pittsburgh School of Medicine, Pittsburgh PA 15261, USA.

ORCiD numbers: 0000-0002-1217-1435 (J.-P.V.), 0000-0003-0484-4596 (L.J.C.), 0000-0003-2180-2136 (A.D.W.), 0000-0002-2168-3344 (I.S.), 0000-0001-9959-4176 (I.B.)

Short title: PTH/PTHrP class B GPCR

Keywords: arrestins; endosomal signaling**;** G protein-coupled receptors (GPCR); location bias; parathyroid hormone; PTH receptor; receptor signaling.

Corresponding author and to whom reprint requests should be addressed:
J.-P. Vilardaga (jpv@pitt.edu)

Grants supporting the writing of the paper: Redaction of this chapter was supported by the National Institute of Diabetes and Digestive and Kidney Disease (NIDDK) of the US National Institutes of Health (NIH) under grant Awards Numbers R01DK116780, R01DK122259, and R21DE032478 (to J.-P.V.), and R01GM139297-01A1 (to I.B.)

Disclosure summary. I.S., J.Y.L., I.B. and J.-P.V. acknowledge potential competing financial interests.

ABSTRACT

The classical paradigm of G protein-coupled receptor (GPCR) signaling via G proteins is grounded in a view that downstream responses are relatively transient and confined to the cell surface, but this notion has been revised in recent years following the identification of several receptors that engage in sustained signaling responses from

subcellular compartments following internalization of the ligand-receptor complex. This phenomenon was initially discovered for the parathyroid hormone (PTH) type 1 receptor (PTH_1R), a vital GPCR for maintaining normal calcium and phosphate levels in the body with the paradoxical ability to build or break down bone in response to PTH binding. The diverse biological processes regulated by this receptor are thought to depend on its capacity to mediate diverse modes of cAMP signaling. These include transient signaling at the plasma membrane and sustained signaling from internalized PTH_1R within early endosomes mediated by PTH. Here we discuss recent structural, cell signaling and *in vivo* studies that unveil potential pharmacological outputs of the spatial versus temporal dimension of PTH_1R signaling via cAMP. Notably, the combination of molecular dynamics (MD) simulations and elastic network model (ENM)-based methods revealed how precise modulation of PTH signaling responses is achieved through structure-encoded allosteric coupling within the receptor between the peptide hormone binding site and the G protein coupling interface. The implications of recent findings are now being explored for addressing key questions on how location bias in receptor signaling contributes to pharmacological functions, and how to drug a difficult target such as the PTH_1R toward discovering nonpeptidic small molecule candidates for the treatment of bone and mineral metabolism diseases.

1. The Role of PTH_1R in Human Health

The parathyroid hormone (PTH) type 1 receptor (hereafter referred to as PTH_1R) is a G protein-coupled receptor (GPCR) and the canonical cell surface receptor for PTH and PTH-related protein (PTHrP) (1). Secreted as an 84-amino acid peptide, PTH is the quintessential regulator of ionized serum calcium (Ca^{2+}) and phosphate (PO_4^{3-}) levels in the body (**Fig. 1A**). In response to hypocalcemic conditions when Ca^{2+} concentration falls below the homeostatic set point in blood, or approximately 1.2 ± 0.1 mM, PTH is secreted from the parathyroid glands and acts in an endocrine fashion by exerting effects on specific bone and kidney cells to adjust the balance of calcium and phosphate ions, and regulate bone remodeling (2,3). In bone, PTH-mediated activation of the PTH_1R expressed by osteoblasts and osteocytes ultimately promotes bone

matrix resorption and liberation of Ca^{2+} into the systemic circulation (4-7). In the kidneys, PTH increases Ca^{2+} reabsorption by distal tubule cells by modulating expression and activity of Ca^{2+} transport proteins (8,9). Concomitant with this effect of PTH is a decrease in inorganic phosphate reabsorption in proximal tubule cells via reduction of cell surface sodium-dependent phosphate transporters (10-12), which ensures that Ca^{2+} remains in the ionized state. PTH also acts on renal proximal tubule cells to increase circulating levels of active vitamin D3 (VitD) via upregulation of the 25-hydroxyvitamin D3 1α-hydroxylase, and active VitD subsequently serves to increase absorption of Ca^{2+} from the gastrointestinal tract. PTHrP is secreted as a 139-, 141-, or 171-amino acid protein that is capable of inducing analogous effects on bone and kidney cells observed for PTH, which is not surprising given the shared amino acid sequence homology within the N-terminal region of these peptides that has been shown to be critical for activity (13-15). While it was originally associated as a factor responsible for the hypercalcemia frequently observed in cancer patients, PTHrP is now recognized to play a role in the growth and development of a variety of tissues, including bone (16), mammary glands (17), and teeth (18). PTHrP mostly acts in a paracrine manner on numerous tissues, including bone, growth plate, and mammary gland during development (15,19). While native PTH is constituted of 84 amino acids and PTHrP consists of splice variants of 139, 141, and 173 amino acids, synthetic or recombinant N-terminal fragments $PTH_{1–34}$ (also known as teriparatide) and $PTHrP_{1–36}$ maintain full activity and are primarily used in research studies (14,20-22) (**Fig. 1B**).

Abnormalities in PTH_1R signaling cause a variety of diseases, previously reviewed in detail (23). In brief, the lack of a functional PTH_1R, such as through expression of homozygous inactivating PTH_1R mutants, causes fetal mortality in Blomstrand Chondrodysplasia (24,25). Heterozygous expression of inactive PTH_1R can cause enchondromatosis/Ollier disease, in which patients develop benign cartilaginous tumors (26), or primary failure of tooth eruption (27,28). Conversely, heterozygous constitutively active PTH_1R variants with a single mutation in the transmembrane (TM) helices 2 (H223R), 6 (T410P), or 7 (I458R) cause Jansen's

metaphyseal chondrodysplasia, a very rare disease characterized by short-limbed dwarfism and hypercalcemia (29-31).

Anomalous hormone levels also trigger severe diseases associated with PTH_1R functions. PTHrP hypersecretion from tumoral cells induces excessive PTH_1R activity, leading to humoral hypercalcemia of malignancy (HHM) encountered in ≈ 25% of cancer patients (32). Over or under secretion of PTH causes hyper- and hypoparathyroidism, respectively. Hyperparathyroidism treatment typically involves surgical removal of the parathyroid glands (33) or pharmaceutical therapy by calcimimetics (allosteric activators of the calcium-sensing receptor, a class C GPCR) to reduce PTH secretion by parathyroid glands. Patient intolerance and the risk of hypocalcemia associated with parathyroidectomy, however, limit these approaches. Current treatment of hypoparathyroidism includes oral calcium, active VitD, and daily subcutaneous administration of recombinant human $PTH_{1–34}$ or PTH (34).

While continuous infusion of PTH was found to promote net bone catabolism (2,35), intermittent $PTH_{1–34}$ injections promote net bone anabolism and are used to treat osteoporosis (36-38). A synthetic analog of $PTHrP_{1–34}$, abaloparatide (ABL) (**Fig. 1B**), was recently developed to treat postmenopausal women with osteoporosis (39). Recent studies have reported that ABL can be more effective than teriparatide at promoting bone formation while reducing the hypercalceimic effect (39-42). The molecular basis for the differing capacity of these ligands to engage a calcemic response in human is unknown but may be related to differences in their binding mode to the PTH_1R. Studies in cultured cells expressing the recombinant PTH_1R show that PTH_{1-34} and ABL stabilize different PTH_1R conformations (21,43). This ligand-dependent PTH_1R conformation selectivity is thought to cause distinct residence time ($1/k_{off}$ where k_{off} is the dissociation rate constant) of ligands to the receptor (prolonged for PTH_{1-34}) (21), which in turn alters the spatiotemporal mode of PTH_1R signaling, an emerging paradigm discussed in the following paragraphs.

2. The PTHR Signaling Paradigm

2.1 GPCR signaling

All GPCRs share a common structural architecture: a hallmark transmembrane domain (TMD) consisting of seven membrane spanning α-helices connected by three extracellular loops and three intracellular loops, N-terminal (extracellular) and C-terminal (cytoplasmic) portions that differ between GPCR families. Based on sequence and functional analyses, human GPCRs are classified into five families: glutamate, rhodopsin, adhesion, frizzled, and secretin families, as defined by the International Union of Basic and Clinical Pharmacology (IUPHAR) "GRAFS" classification (44,45).

Most prominent members of the glutamate receptor family (formerly class C) include metabotropic glutamate receptors, Ca^{2+}-sensing receptor, γ-aminobutyric acid B receptors, and type I taste receptors. The N-terminus of these GPCRs is large and contains the ligand recognition domain composed of two lobes that form a cavity in which ligands bind, altogether reminiscent of the Venus flytrap (VFT) and therefore often referred to as a VFT domain. The VFT domain may also accommodate allosteric binding sites and is connected to the TMD through a cysteine-rich domain, which also plays a role in receptor activation.

The rhodopsin family (also known as class A GPCRs) has the greatest number of members, which typically exhibit small N-terminal regions (46,47). It is comprised of more than 700 receptors that share high sequence similarity (48) and several local structural characteristics with rhodopsin, including an NPXXY motif on TM helix 7 (TM7) and a DRY motif between TM3 and intracellular loop 2 (ICL2) (49). Ligand binding for receptors in this class typically takes place within a cavity formed between TM helices. Notable GPCRs in this class that hold significant physiological relevance include muscarinic acetylcholine receptors, dopamine receptors, adrenergic receptors, opioid receptors, adenosine receptors, and histamine receptors.

The adhesion family has recently attracted much attention due to several unique features. With a sole exception of ADGRA1 (GPR123), these receptors typically possess extremely large extracellular N-terminal domains that contain a highly conserved GPCR autoproteolysis-inducing (GAIN) domain, within which the conserved GPCR proteolysis site (GPS) is located. Autoproteolysis typically takes place in endoplasmic reticulum and generates two fragments, N-terminal (NTF) and C-terminal (CTF), that remain connected via non-covalent interactions. For most adhesion GPCRs (aGPCRs), the N-terminal portion of the CTF, spanning about 15 amino acid residues, comprises a tethered agonist peptide termed *Stachel* sequence. In addition to these characteristic aGPCR features, the N-termini of some of these receptors also contain an abundance of serine and threonine residues that constitute sites for O-glycosylation, which act as mucin-like domains to create rigid structures that protrude from the cell surface and are important in cell-cell adhesion.

The frizzled/taste 2 receptor family is far less understood as compared to other classes, and their similarity is largely confined to results from phylogenetic analysis. Only recently have frizzled receptors been established as true GPCRs following reports that binding of Wnt ligand can induce G protein coupling. Frizzled receptors are characterized by long N-termini with conserved cysteine residues that are considered critical for Wnt binding.

The PTH_1R belongs to the secretin family (or class B GPCR) characterized by a long N-terminus (or extracellular domain, ECD) that adopts a conserved fold composed of two major elements –an N-terminal α-helix and two antiparallel β-sheets– that are connected by several loops and stabilized by three disulfide bridges. Class B GPCRs bind relatively large peptide hormone ligands that act most often in an endocrine manner rather than a paracrine fashion, with PTHrP as an exception. There are currently 15 identified members of this family in humans (50).

In the conventional paradigm for understanding GPCR signaling, hormones transmit signals into cells through a series of biophysical and biochemical events that are initiated at the

plasma membrane by ligand binding to a receptor (51,52). This first event stabilizes the active receptor conformation that couples to and activates heterotrimeric G proteins. G protein activation involves release of the guanosine-5'-diphosphate (GDP) molecule bound to the Gα subunit of the G protein and the binding of a guanosine-5'-triphosphate (GTP); in this way, the activated GPCR acts as a guanine exchange factor (GEF). Since the concentration of GTP is several-fold higher than that of GDP in cells, GTP readily binds to nucleotide-free Gα (53). GTP binding triggers the dissociation or rearrangement of Gα from the Gβγ heterodimer thus permitting Gα-GTP and Gβγ to independently regulate activities of membrane–bound enzymes and ion channels, respectively. There are four main classes of Gα subunits that have been identified based on sequence similarity (54): G_s that stimulates adenylyl cyclase activity to increase intracellular cyclic adenosine monophosphate (cAMP) levels; $G_{i/o}$ that inhibits adenylyl cyclase activity; $G_{q/11}$ that leads to an increase in intracellular Ca^{2+} levels via activation of phospholipase C (PLC) β; and $G_{12/13}$ that regulates Rho guanine nucleotide exchange factors.

Each G protein subunit contains distinct domains that play specific roles during GPCR signaling. The Gα subunit consists of GTPase and flexible α-helical domains (55). In the presence of nucleotides, the GTPase domain binds and hydrolyses GTP to GDP, while the helical domain forms a lid over the nucleotide binding site (53,56). There are five subtypes of Gβ and twelve subtypes of Gγ subunits expressed in humans (57). The Gβ subunit adopts a β-propeller structure with seven blades along with a long α–helical N-terminus (55), whereas Gγ consists of two α-helical segments, which strongly bind to the N-terminal helix and to the blades 1, 4–7 of Gβ. While the specific actions of each subtype combination are under investigation, the $Gβ_1γ_2$ heterodimer is ubiquitously expressed and regulates many effectors, including several adenylyl cyclase subtypes, ion channels, and phosphoinositide 3-kinase gamma (PI3Kγ) (57,58). Within seconds after agonist binding, the activated receptor interacts with GPCR kinases (GRKs) that initiate receptor desensitization by: 1) preventing G protein coupling (59),

and 2) receptor phosphorylation which engages or stabilizes receptor association with β-arrestins (β-arrestin 1 and β-arrestin 2) to promote internalization of the receptor–arrestin complex into endosomes (60-63). Such receptor desensitization leads to the termination of G protein-mediated downstream signaling and reassociation of subunits into the heterotrimeric complex (64). Following receptor internalization to endosomes, the agonist dissociation ensues, and the receptor can be either targeted to lysosomes for degradation (referred to as receptor downregulation) or dephosphorylated and recycled back to the plasma membrane for a new cycle of activation and signaling (referred to as receptor resensitization) (65).

2.2. Paradigm shift in PTH_1R signaling via G proteins

The PTH_1R predominantly activates G_s and $G_{q/11}$ in response to PTH or PTHrP binding. G_s activates adenylyl cyclases resulting in the production of cAMP and PKA activation (1,66), whereas the $G_{q/11}$ ($G\alpha_q$, $G\alpha_{11}$) subfamily activates phospholipase Cβ (PLCβ), which then cleaves phosphatidylinositol (4,5)-bisphosphate (PIP_2) to generate diacylglycerol (DAG) and inositol (1,4,5)-trisphosphate (IP_3). IP_3 activates calcium channels at the endoplasmic reticulum, releasing stored Ca^{2+} into the cytosol, while DAG activates protein kinase C (PKC). The PTH_1R can also activate the $G_{12/13}$ subfamily ($G\alpha_{12}$, $G\alpha_{13}$), which engages the phospholipase D/RhoA signaling pathway (67,68), and Gi (69).

Back in the 00s, it was well established that PTH_{1-34} infusion stimulates significant increases in serum Ca^{2+}, serum Vitamin D in its active form (i,e., 1,25-dihydroxyvitamin-D3), urinary phosphate ion (PO_4^{3-}), and bone resorption. However, it was unclear why these physiological parameters were not increased at a comparable dose of $PTHrP_{1-36}$ infusion given that PTH and PTHrP share similar pharmacological properties as they relate to binding affinity and stimulation of cAMP production (**Fig. 2A**, **B**) (70)**.**The development and application of quantitative Förster resonance energy transfer (FRET)-based approaches to determine kinetics and rate-limiting reactions for each

step along the PTH_1R signaling cascade at the single-cell level (reviewed in (71) unveiled signaling differences between PTH_{1-34} and $PTHrP_{1-36}$ and a new mode of GPCR signaling via cAMP. Ligand–PTH_1R interaction and cAMP production measured by FRET showed that $PTHrP_{1-36}$ binding is fully reversible and induces transient cAMP after ligand washout, whereas PTH_{1-34} remains bound and induces sustained cAMP generation (**Fig. 2C**). Knowing that PTH induces rapid PTH_1R internalization (72-74), the protracted cAMP response is inconsistent with the conventional model of GPCR desensitization as G protein-dependent signaling by activated receptor is quickly terminated following receptor phosphorylation by GRKs and the recruitment of β-arrestins, which both sterically occlude G protein binding and promote endocytosis of ligand-bound GPCRs. Thus, signaling responses by GPCRs were initially considered transient in nature and confined to the plasma membrane**.** However, this model has been revised in recent years after the observation that blocking PTH_1R internalization prevents the sustained cAMP response (75,76) (**Fig. 3A,B**) and that PTH mediates sustained cAMP signaling from early endosomes following internalization of a ternary PTH_1R–Gβγ–βarrestin complex (**Fig. 3C**) (77). This unexpected aspect of PTH_1R signaling is due to the apparent ligand-dependent nature of endosomal signaling by this receptor and will be discussed in the next section. Notably, the production of two distinct pools of cAMP has been verified for several other GPCRs in class A and class B (76,78,79) and reviewed in (80) and is now considered an integral part of GPCR signaling (81).

2.3 Mechanisms of Endosomal PTH_1R signaling via cAMP and its regulation

Two distinct active PTH_1R conformations are thought to be responsible for the distinct duration of cAMP production (20,71). The binding affinity of one of the conformations, referred to as the R^0 conformation, is independent of G protein coupling. The R^0 conformation is preferentially stabilized by PTH and maintains cAMP production when the receptor internalizes in early endosomes. The second conformation, referred to as the R^G conformation, corresponds to the

classical G protein-dependent high-affinity receptor, which is indistinguishably stabilized by PTH or $PTHrP_{1-36}$. Accordingly, whereas the R^G conformation stabilized by $PTHrP_{1-36}$ is G protein-dependent and is associated with transient cAMP responses from the plasma membrane, the R^0 state is not altered by G protein coupling but nevertheless permits sustained cAMP generation following internalization of the receptor (20,76,82,83). The C-terminal portion of PTH (i.e., residues 15–34) plays a critical role in receptor selectivity and affinity by binding to the PTH_1R extracellular domain (PTH_1R^{ECD}) (84,85). Structural studies revealed a perfect alignment for peptides containing the same C-terminal 15–34 amino acid residues, i.e. ^{C}PTH-type including PTH and ePTH (a mimetic PTH agonist where PTH amino acid residues 1,3,10,11,12,14,18,34 are replaced with aminocyclopentane-1- carboxylic acid, α-aminoisobutyric acid, Gln, homoarginine, Ala, Trp, norleucine, and Tyr, respectively), or ^{C}PTHrP-type including PTHrP, but C-terminal tips of the ^{C}PTH-type and ^{C}PTHrP-type peptides diverge to opposite sides of $PTHR^{ECD}$ (indicated by arrows in **Fig. 4A**). Such differential binding mode at PTH_1R^{ECD} likely translates to differential overall binding to PTH_1R and results in distinct signaling modes. The N-terminal portion, especially the most N-terminal residues, is critical for PTH_1R signaling, as deletion of PTH Ser1 and Val2 significantly reduces cAMP production (86) (87). Also, PTH_{7-34} acts as a PTH_1R antagonist (88). From sequence analyses, PTH_{1-34} shares several residues and chemical moieties that are not present in $PTHrP_{1-34}$ or ABL, which may be critical for stabilizing the R^0 conformation and inducing sustained cAMP signaling in endosomes; these include Ala1, Ala3, Ile5, Met8, the amide group on residue 10 (**Fig. 1B**). Additionally, Arg11, Ala12 and Trp14 were initially identified in an alanine scanning to increase activity of a short N-terminal PTH fragment that was referred to as modified-PTH_{1-14} (M-PTH_{1-14}) (89-92). Further optimization of the signaling properties of M-PTH_{1-14} resulted in the chimeric peptide M-PTH_{1-34}, which binds the the R^0 conformation of PTH_1R with high affinity and trigger prolonged elevation of serum Ca^{2+} (sCa) when injected subcutaneously into mice (82). Additional structure-activity studies to improve the solubility of this peptide by substitution of C-terminal hydrophobic PTHrP

residues Leu18, Phe22 and His26 by Ala, Ala and Lys, respectively, resulted in the [Ala^{18,22},Lys^{26}]-M-PTH$_{1-14}$/PTHrP$_{15-36}$ peptide referred to as LA-PTH, which maintains a higher affinity binding to the PTHR R^0 conformation than PTH, and sustains endosomal cAMP signaling at time points by which PTH has dissociated from the receptor (93,94). Given the high affinity and residence time of LA-PTH (43,83,95) for PTH$_1$R, this ligand was used to solve high-resolution cryo-EM structures of PTH$_1$R in complex with G$_S$ that will be discussed in part 3.

In the case of PTH$_1$R, a ternary complex composed of PTH-bound PTH$_1$R, β-arrestin, and Gβγ is required for endosomal cAMP production. The mechanism by which this ternary complex maintains production and elevated levels of cAMP was studied in cells expressing recombinant or native PTH$_1$R and proceeds as follows (**Fig. 5A-C**). First, it promotes the activation cycle of G$_s$ from endosomes (77). Second, it activates extracellular signal-regulated protein kinase 1/2 (ERK1/2) via β-arrestins thus reducing the activity of the cAMP-specific phosphodiesterase PDE4 (96). Third, it stimulates the conditional activation of adenylate cyclase type 2 via Gβγ (94). Following the recognition of these functional roles, White *et al.* (97) have demonstrated that G$_q$ activation by PTH is determinant in the formation of the ternary PTH$_1$R–Gβγ–arrestin complex. Gβγ released upon G$_q$ activation promotes the conversion of PI(4,5)P$_2$ to PI(3,4,5)P$_3$ by phosphoinositide 3-kinase β (PI3K$_\beta$), which in turn promotes β-arrestin recruitment to PTH$_1$R and formation of the ternary receptor complex (**Fig. 5B,** steps 3 and 4).

Termination of the sustained cAMP response by the PTH$_1$R is predominantly controlled by mechanisms instilled within the endosomal trafficking pathway. Previous work has highlighted that the release of β-arrestins from the PTH$_1$R localized in endosomes is concomitant with association of the retromer complex with the receptor (96) (**Fig. 5D**). The retromer complex is comprised of two membrane-bound sorting nexins (SNX1 and SNX2) as well as a heterotrimer consisting of vesicle protein sorting (Vps) 26, 29, and 35, which

collectively serve to regulate the sorting of cargo proteins from early endosomes to the *trans*-Golgi network (98,99). Examination of this complex in the context of PTH_1R-mediated cAMP showed that overexpression of Vps subunits reduces the duration of cAMP generation, whereas siRNA targeting of the subunits prolonged cAMP signaling time courses (96). This process was recently shown to be dependent upon a negative feedback loop in which activated PKA increases the proton pump activity of endosomal membrane-bound v-ATPase, resulting in endosomal acidification (100). The decrease in endosomal pH then leads to the disassembly of the signaling PTH_1R–$G\beta\gamma$–arrestin complex and concomitant assembly of inactive PTH_1R with the retromer, forming a complex that traffics to the Golgi apparatus (96,100) and/or engages receptor recycling back to the plasma membrane (**Fig. 5D**) (100).

3. Structural characterization of PTH_1R

As for many class B GPCRs, the crystal structure of the isolated PTH_1R^{ECD} was first resolved either in the absence or presence of ligands (84,85,101). These structures demonstrate direct interaction between the C-terminal portion of peptide ligands and the receptor ECD and provide snapshots of the first step in peptide ligand binding to its receptor (**Fig. 4A**). High resolution structures of PTH_1R were then solved by different approaches concomitantly. An inactive signaling conformation of PTH_1R was crystallized with a mimetic PTH agonist ePTH (102) (**Fig. 4B**). **T**he receptor is maintained in an inactive state via a dense interaction network (cyan dashes in **Fig. 4B**) sealing TM6 to the core of the receptor (see detailed in a close-up view, where interacting residues are shown in stick representation). The conserved PxxG motive in the middle of TM6 (highlighted in red with $P415^{6.42b}$ in **Fig. 4B**) faces outward and away from inactive-state stabilizing network; however, these observations need confirmation given that stabilizing mutations and fusion protein inserted in ICL3 of the receptor construct used for crystallization likely contribute to the inactive receptor state. Three fully active conformations (referred to as states 1–3) of LA-PTH-bound PTH_1R in complex with G_s were determined by

cryo-EM (87) (**Fig. 6**)**.** LA-PTH interactions with PTH_1R involve a continuous α-helix connecting the PTH_1R^{ECD} and the transmembrane domain (PTH_1R^{TMD}), as seen in other published structures of class B GPCR–G_s complexes (103-106). Specifically, the C-terminal residues 18–34 of LA-PTH are dissociated from the PTH_1R^{ECD} in the state 3 structure (**Fig. 6**) suggesting that residues at the C-terminus of the peptide can undergo many dissociation-rebinding cycles while in complex with PTH_1R. Contacts between peptide residues 1–14 and the receptor TMD are likely critical for maintaining active peptide–receptor complex during dissociation and possibly re-association events of the C-terminal peptide part.

From these data, a hypothetical model for sustained endosomal signaling by LA-PTH can be proposed in which the large number of contacts between LA-PTH and PTH_1R^{TMD} (shown as cyan dashed lines in **Figure 4D**, left close-up view) reduce ligand dissociation at endosomal pH, despite dissociation of the peptide C-terminal part. In contrast, the destabilization of PTH–PTH_1R at endosomal pH leads to the release of PTH from the receptor and termination of signaling (100) (step 9 in **Fig. 5D**).

To date, structures of nearly all class B GPCRs in active G_s-coupled states have been solved refs (107-117) and display a common structural feature – a sharp outward kink in the middle region of TM6, which opens the receptor cytosolic interface for coupling to G proteins or β-arrestins. Such hallmark feature is also present in active state PTH_1R structures (87) (**Fig. 4C,D**) and is the most pronounced structural rearrangement occurring when the receptor switches from the inactive to its fully active state as highlighted in **Figure 4C**. In particular, the $P415^{6.42b}$ of the conserved class B GPCR PxxG motif faces away from TMD core in an inactive state but is twisted inwards in the active state and engages in interactions with $Q451^{7.45b}$ and $V455^{7.49b}$ on TM7 (see close-up view in **Fig. 4C**), overall resulting in partial unwinding of a portion of TM6 above (C-terminal to) the PxxG motif and a large outward movement of the lower part of TM6 N-terminal to the PxxG motif (red continuous arrow in **Fig. 4C**) (112). This results in

formation of a sharp kink in the middle of TM6 of fully active PTH_1R and a large opening of receptor's cytosolic core for G protein binding. In addition, PTH_1R^{ECD} may also undergo rearrangement of its position with respect to TMD to adapt the peptide ligand into TMD for receptor activation (dashed red arrow in **Fig. 4C**); the type, extent and stability of such motion might be dependent on the type of peptide ligand agonist.

Other structural rearrangements upon receptor activation also include minor reorganization in the extracellular portions of TM1 and TM7 move toward TM6 in the active state receptor. The other TM helices also exhibit shifts, mostly outward from the receptor core upon activation. These structural rearrangements may contribute to the outward TM6 kink (112). Comparing active state cryo-EM structures with the inactive state crystal structure shows that the first three residues of LA-PTH push against TM6, and ligand residue Glu4 stabilizes an extensive polar core network within the receptor (**Fig. 4D**, left close-up), both of which promote the outward TM6 kink characteristic of receptor activation. The large outward movement of TM6 is required and presumably induced and stabilized by $G\alpha_s$ subunit binding via interactions of its C-terminal α5-helix (highlighted green in **Fig. 4D**) with the receptor's cytosolic core. Such profound movement of TM6 to open cytosolic core of class B GPCRs likely is not induced by agonist peptide binding alone. Recent cryo-EM studies of calcitonin-gene-related peptide receptor (CGRPR) in apo and CGRP-bound states revealed that CGRP-bound and apo receptor structures are highly similar (118). Agonist binding increases structural dynamics at lower halves of TM5 and TM6 in CGRP-bound receptor indicating that agonist binding destabilizes inactive-state interaction networks, and this is required for effective G protein coupling eventually leading to a sharp kink formation in receptor'sTM6 and full opening of cytosolic core. Such activation mechanism is likely common among all class B GPCRs.

4. PTH binding to PTHR: a structure-encoded allosteric mechanism

The binding of PTH to PTH_1R proceeds via a two-step association mechanism (119). The molecular model of this two-step reaction is displayed in **Figure 7**. In the first step, the C-terminal part of the ligand (residues 16–34) rapidly binds to the receptor N-extracellular domain (PTH_1R^{ECD}) following bimolecular reaction kinetics, defined by $k_{obs} = k_{off} + k_{on}[L]$, where k_{obs} is the measured rate constant (s^{-1}), and k_{on} and k_{off} are the association and dissociation rate constants, respectively, and [L] is the ligand concentration. In the second and slower step, the N-terminal part of the ligand (residues 1–15) binds to the receptor TMD (PTH_1R^{TMD}) via a complex reaction involving a bimolecular interaction coupled to conformational changes in both peptide hormone and receptor. This reaction follows a hyperbolic dependence on hormone concentration.

NMR experiments titrating unlabeled purified PTH_1R^{ECD} into a sample of ^{15}N-labeled $PTH_{1–34}$ provided further insights on the molecular mechanism of this complex reaction (120). In brief, the binding of the PTH C-terminal part to PTH_1R^{ECD} triggers a distinct and more structured conformation in the N-terminal region of $PTH_{1–34}$ independent of the interaction with PTH_1R^{TMD}, which in turn primes this N-PTH region for interaction with PTH_1R^{TMD} and resulting in a continuous PTH helix conformation. Such placement of the PTH N-terminal part, especially of residues 1–4, stabilizes the active receptor conformation, given that N-terminal PTH residues 1–4 are essential to trigger activation of G_s proteins and cAMP production (87).

Toward elucidating the allosteric changes in PTH_1R structure triggered by PTH binding, we examined the spectrum of conformational motions, or thermal fluctuations (also called Brownian motions), accessible to the PTH–PTH_1R complex embedded in a lipid bilayer (120). The spectrum comprises a wide range of relaxational motions, from low frequency modes that cooperatively engage the entire structure to those, in the high frequency regime, that are highly localized (121). Several studies have demonstrated that the low frequency modes of motions, robustly defined by the overall architecture, represent cooperative changes in structure that are

often required for biological function, including allosteric activation (122). The mode spectrum can be uniquely determined for each structure by normal mode analysis. We analyzed that of the PTH–PTH_1R complex using an extension of the anisotropic network model (123) (ANM) that takes into account the constraints exerted by the lipid bilayer implemented in the *DynOmics* server (124), and we focused on the most cooperative movements predicted for the complex. Our analysis revealed the predisposition of the complex to a cooperative motion, which enables the 'opening' of the intracellularly exposed ends of TM5 and TM6 and the connecting intracellular loop ICL3 (Movie S1 and **Fig. 8A, B**), reminiscent of the activated state of class B GPCRs (see **Fig. 4D**), suggesting that the conformational transition triggered by ligand binding can readily induce a structural change at the cytoplasmic ends of TM5 and TM6.

To visualize more clearly the coupling between the PTH binding site and the cytoplasmic regions that undergo large rearrangements, we analyzed the cross-correlations between (PTH and PTH_1R) residue motions in this mode. The results are presented as a heat map in **Figure 8C**. The *red blocks* indicate the structural elements that undergo highly correlated movements, and the *blue blocks* indicate the pairs of structural elements that undergo anticorrelated (opposite direction) fluctuations. We focused on the type and strength of coupling between the PTH N-terminal residues S1-H14 inserted into the PTH_1R^{TMD} (**Fig. 8D**; *orange ellipse*) and the ICL3 connecting TM5 and TM6, using T392 located at the cytosolic tip of TM6, as a reference point for probing conformational rearrangements associated with receptor activation. The heat map clearly showed that PTH V1-H14 was strongly correlated with TM5-ICL3-TM6, as well as the extracellularly exposed region of TM1. Furthermore, examination of the correlation between T392/ICL3 and all PTH_1R residues (*vertical rectangular box* in **Fig. 8C** and *ribbon diagram* in **Fig. 8D** color-coded by these correlations) showed that T392 belongs to a highly coherent block encompassing the substructure from approximately the mid-part of TM5 all the way to its cytoplasmic end, the entire TM6 and the N-terminal half of TM7 (up to F447), in strong support

of the coupling of this entire substructure to PTH S1-H14. This highly coupled region is naturally expected to allosterically transmit the perturbations at the PTH binding site to the TM5-ICL3-TM6 cytoplasmic region.

5. PTH_1R Druggability

Overall, ANM analysis (or its extension ESSA (125) implemented in the interface *ProDy*) unveils the structural elements that mediate the allosteric signaling properties of target proteins. Recent application to PTH_1R, in conjunction with druggability simulations, pointed to an allosteric and druggable region in the vicinity of the extracellular ends of TM1 and TM2 (126). In particular, the TM1 residues E180 and R181 were distinguished by their high affinity for binding drug-like probe molecules. Pharmacophore modeling using snapshots from druggability simulations, followed by virtual screening of libraries of small molecules led to the identification of a series of small molecules. One of these small molecules, Pitt12, was experimentally verified to act as a negative allosteric modulator (NAM) of PTH_1R (126). The binding pose of Pitt12 onto LA-PTH-bound PTH_1R observed in MD simulations, as illustrated in **Figure 9A**, displays the particular atoms engaged in highly stabilizing interactions with selected E180 and R181 atoms (**Fig. 9B**). Notably, a recently resolved positive allosteric modulator (PAM) of the glucagon-like peptide 1 (GLP-1) receptor (GLP_1R), another Class B GPCR mentioned above, also binds the same site, but this modulator (LSN3160440) inserts slightly deeper into the TMD. The structural alignment of the allosteric modulator binding sites for Pitt12-bound PTH_1R and LSN3160440-bound GLP_1R (**Fig. 9C**) supports the view that the interfacial region between the N-terminal region of TM1 and the bound peptide or substrate (here LA-PTH and GLP-1) harbors a site with a high propensity to bind allosteric small molecules that might be a common allosteric druggable site among all class B GPCRs. The allosteric effect of ligand binding to this site is consistent with the highly cooperative interaction between the PTH N-terminal residues, the cytoplasm-exposed

halves of TM5 and TM6 and connecting loop ICL3, and the N-terminal extracellularly exposed end of TM1 noted in **Figure 8D**. Although Pitt12 and LSN3160440 share a similar binding site and pose in their respective receptors, these small allosteric molecules produce opposite modulation of receptor signaling via G_S/cAMP. In the case of LSN3160440, it acts as a PAM by stabilizing the interaction of $GLP1_{9-36}$ for the active GLP_1R conformation (127). In the case of Pitt12, molecular dynamic simulations predict that it operates by shifting the position of the PTH_{1-34} peptide's N-terminal tip resulting in an outward displacement of TM5 and TM6 helices; this conformational rearrangement would be consistent with the NAM activity of Pitt12 in reducing PTH_1R coupling to G protein. Another non-peptidic molecule, PCO371, acting as agonist for the PTH_1R with a µM potency for the stimulation of cAMP in cells expressing the recombinant at PTH_1R has been previously discovered (127). The binding site is not resolved and initial phase 1 clinical trials to test this molecule as a potential orally available drug candidate for the treatment of hypoparathyroidism (hypocalcemia) have been terminated (128,129). Acting as a NAM, Pitt 12 is under optimization for improving its efficacy and potency as a potential candidate for future treatment of bone and mineral diseases linked to PTH_1R hyperactivity due to hypersecretion of PTH or PTHrP encountered in hyperparathyroidism or in hypercalcemia of malignancy, respectively.

6. Location bias in PTH_1R signaling and pharmacological implications

Sustained endosomal cAMP production has likely important pharmacological and physiological implications, as injection of LA-PTH into mice and monkeys increases serum calcium and decreases serum phosphate more efficiently than does $PTH_{1–34}$ (83,95). Conversely, a PTH mutant (PTH-R25C) found in patients with a severe form of chronic hypocalcemia cannot stimulate endosomal PTH_1R signaling via cAMP in cells and fails to elevate blood Ca^{2+} elevation

in animals (21,130) (**Fig. 10A**). The recent (2021) design of a novel PTH_{1-34} variant contributed to better understand the functional role of location bias (plasma membrane vs endosmes) in PTH_1R signaling independently of the duration of cAMP. The ANM analysis of inter-residues cross-correlations in the PTH-bound receptor (**Fig. 8C**) let to conceive a PTH analog via epimerization of Leu 7 (PTH^{7d}) with the desired bias property to sustain cAMP production exclusively from the plasma membrane (131). Findings from studies in cells and mice comparing the effects of the two biased PTH agonists, PTH^{7d} and LA-PTH that induced a similar elevation and duration of cAMP production but generated in separate cell locations –plasma membrane (for PTH^{7d}) *vs* endosomes (for LA-PTH)– helped examine the role of location bias in cAMP production for prime pharmacological functions of the PTH_1R (131) (**Fig. 10B**). In mice, LA-PTH and $PTH7^d$ injections led to a similar reduction in serum phosphate ion due to inhibition of renal phosphate reabsorption (a major physiological role of PTH acting via PTH_1R to maintain plasma PO_4^{3-} level constant), however, LA-PTH induces significantly more elevation of serum Vitamin D and Ca^{2+} than PTH^{7d} (**Fig. 9B**). In polarized Mardin-Darby canine kidney cells, LA-PTH generated endosomal cAMP pool ensures nuclear cAMP accumulation and nuclear PKA activity leading to production of the 25-hydroxyvitamin D 1-α-hydroxylase (1α[OH]ase), the rate-limiting enzyme catalyzing the formation of active Vitamin D. Conversely, the PTH^{7d}-generated plasma membrane cAMP pool does not lead to nuclear PKA activity and elevation of the 1α[OH]ase. These observations support possible functional implications of distinct locations of cAMP generation in the control of mineral-ion balance and Vitamin D levels.

7. PTH_1R coupling to β-arrestins

7.1 Binding mode of arrestin to GPCRs

Arrestins engage with activated GPCR at two main sites: 1) a positively charged groove located in the N-terminal domain of arrestin binds to the phosphorylated C-terminal tail (C-tail) of the

receptor; 2) several regions, including a finger loop, interact with the receptor core (132,133). Binding of phosphorylated receptor C-tail to arrestin displaces the arrestin C-tail, disrupting a three-element interaction and a polar core that stabilize the inactive arrestin conformation (134). These changes promote an active conformation in which the N- and C-terminal domains are rotated by 20°. The arrestin finger loop adopts a helical conformation upon engagement with the receptor core (135). Residues in the finger loop, lariat loop, and elsewhere on arrestin form hydrophobic and polar interactions with the receptor core. In comparison with an arrestin structure bound to a synthetic receptor phospho-peptide, the structure of rhodopsin (the light-sensing GPCR)-bound arrestin (135) exhibits unique loop conformations and a small change in the interdomain twist. While binding to the receptor C-tail was previously considered a prerequisite for engagement with the receptor core (132), recent research suggests that arrestin can also engage with the receptor core independent of receptor C-tail engagement (136,137). Extensive molecular dynamics (MD) simulations of rhodopsin–arrestin-1 complex determined that interactions between arrestin loops, not including the finger loop, with receptor intracellular loops (ICL) 2 and 3 are the main mediators of arrestin activation via the receptor core. Furthermore, both receptor core and phosphorylated C-tail binding trigger arrestin activation by promoting distinct conformations of arrestin C-loop and lariat loop. While the molecular mechanism of arrestin C-tail displacement is not clear, the displaced C-tail binds clathrin and clathrin adaptor AP2, permitting receptor internalization (62,137,138).

7.2 PTH_1R–arrestin interaction

Part of the contact residues between PTH-activated PTH_1R and β-arrestin-1 (βarr1) have been identified using photo-crosslinking coupled to mass spectrometry (MS) experiments (139). Crosslinks between residue Leu73 in the finger loop of βarr1 and PTH_1R residues $K405^{6.32b}$, $K408^{6.35b}$, and $K484^{8.68b}$ are formed in response to $PTH_{1–34}$. PTH_1R residues $K405^{6.32b}$ and

Lys408$^{6.35}$ are located at the cytoplasmic end of TM6, while K484$^{8.68b}$ is located within the flexible C-terminal tail and is not visible in the cryo-EM structure of PTH_1R (87). Crosslinks were also identified between F75 of βarr1 and PTH_1R residues V384$^{5.64b}$ and T392$^{5.71b}$, located at the cytoplasmic end of TM5. These photo-crosslinks support a conformation in which the βarr1 finger loop is engaging with the receptor cytosolic core as observed in the crystal structure of rhodopsin bound to the murine visual arrestin (140).

To visualize these photo-crosslinks, models of PTH_1R bound to βarr1 were generated using MD snapshots of PTH_1R (120) and three structures of GPCR–arrestin complexes: rhodopsin–visual arrestin (PDB 5W0P, Model 1) (135), M2 muscarinic receptor–βarr1 (PDB 6U1N, Model 2) (141), and neurotensin receptor 1–βarr1 (PDB 6UP7, Model 3) (142) (**Fig. 11**). PyMOL was used to perform structural, sequence-independent alignment of the TMD of the GPCR–βarr1 template structure to the PTH_1R^{TMD} (residues 180–460) from each snapshot. In the model of PTH_1R–βarr1 complex generated using rhodopsin–visual-arr (Model 1) (135), C-edge loops are slightly embedded in the membrane (**Fig. 11A**), as observed in other GPCR–arrestin structures (135,141-143). The βarr1 in Model 3 clashes significantly with the membrane (**Fig. 11C**), and interactions between PTH_1R helix 8 residues and the membrane are eliminated (**Fig. 11D,E**). Model 1 satisfies distance restraints between residues Leu73 and K484$^{8.68b}$ of βarr1 and PTH_1R, respectively, as well as the position of phosphorylated receptor C-terminal tail within the N-terminal domain of βarr1. Additionally, Cα–Cα distances between βarr1 Leu73 and PTH_1R K405$^{6.32b}$/K408$^{6.35b}$ as well as between βarr1 F75 and PTHR V384$^{5.64b}$/T392$^{5.7b}$ are well within photo-crosslinking restraints (**Fig. 11A**). The inward movement of receptor TM6 relative to the G_s-bound conformation has been reported essential for βarr coupling (144). The PTH_1R–βarr1 model permits this TM6 inward movement without clashing with βarr1. Interface in this PTH_1R–βarr1 complex (Model 1) includes many contacts with ICL1 and ICL2, more so than in Model 2 (**Fig. 11B**).

8. Next questions to address

Ongoing basic research is providing important insights into structural mechanisms of PTH_1R signaling in response to PTH and PTHrP, including ligand binding, receptor activation, and coupling to G_s and β-arrestins. Since its initial discovery, significant advancements have been made toward elucidating the molecular and cellular determinants that underlie PTH_1R endosomal cAMP. Even so, several outstanding questions remain. Although we made models of PTH_1R–βarr based on available structures, conformational heterogeneity in GPCR–arrestin complexes has been observed (142). Cryo-EM analysis of 2D class averages from purified PTH_1R–βarr could reveal possible conformations of this complex. Importantly, it is not clear what are the structural differences are between PTH_1R–arrestin complexes at the plasma membrane versus those in endosomes (i.e., supercomplex with both β-arrestin and G_s bound). What structural features contribute to PTH_1R coupling to G_q and $G_{12/13}$? Also, how does PTHrP/ABL stabilize unique conformations of PTHR that lead to transient cAMP production at the plasma membrane? Recent studies addressed in part this question by showing that $PTHrP_{1-36}$ does not mimic signaling mediated by the native $PTHrP_{1-141}$, which induces sustained cAMP at the plasma membrane due to impaired β-arrestin coupling (145,146). These data motivate a reinterpretation of our prior understanding on how native PTHrP acts on the PTH_1R. Additional structural and cellular studies will also provide a better understanding of the differences in signaling observed between PTH_1R ligands. Do different ligands trigger distinctive membrane lipids dynamics that result in either receptor internalization or retention of receptors at the plasma membrane? Does the ternary PTH_1R–Gβγ–arrestin complex internalize into endosomes whose lipid composition differs when PTH_1R is activated by either PTH_{1-34} or LAPTH? If there is such a difference, does it contribute to the prolonged PTH_1R-LAPTH interaction that engages sustained cAMP? Furthermore, research is needed to determine whether endosomal cAMP

production directly regulates bone turnover. Answering these questions will help explain the differential effects of PTH_1R ligands on bone turnover, calcium levels, and Vitamin D homeostasis and could serve as a foundation for the development of clinically relevant PTH analogs tailored to target specific aspects of PTH_1R signaling involved in bone and mineral diseases.

References

1. Juppner H, Abou-Samra AB, Freeman M, Kong XF, Schipani E, Richards J, Kolakowski LF, Jr., Hock J, Potts JT, Jr., Kronenberg HM, et al. A G protein-linked receptor for parathyroid hormone and parathyroid hormone-related peptide. *Science*. 1991;254(5034):1024-1026.
2. Horwitz MJ, Tedesco MB, Sereika SM, Syed MA, Garcia-Ocana A, Bisello A, Hollis BW, Rosen CJ, Wysolmerski JJ, Dann P, Gundberg C, Stewart AF. Continuous PTH and PTHrP infusion causes suppression of bone formation and discordant effects on 1,25(OH)2 vitamin D. *J Bone Miner Res*. 2005;20(10):1792-1803.
3. Miao D, He B, Lanske B, Bai XY, Tong XK, Hendy GN, Goltzman D, Karaplis AC. Skeletal abnormalities in Pth-null mice are influenced by dietary calcium. *Endocrinology*. 2004;145(4):2046-2053.
4. Silva BC, Costa AG, Cusano NE, Kousteni S, Bilezikian JP. Catabolic and anabolic actions of parathyroid hormone on the skeleton. *Journal of endocrinological investigation*. 2011;34(10):801-810.
5. Boyce BF, Rosenberg E, de Papp AE, Duong LT. The osteoclast, bone remodelling and treatment of metabolic bone disease. *European journal of clinical investigation*. 2012;42(12):1332-1341.
6. O'Brien CA, Nakashima T, Takayanagi H. Osteocyte control of osteoclastogenesis. *Bone*. 2013;54(2):258-263.
7. Saini V, Marengi DA, Barry KJ, Fulzele KS, Heiden E, Liu X, Dedic C, Maeda A, Lotinun S, Baron R, Pajevic PD. Parathyroid hormone (PTH)/PTH-related peptide type 1 receptor (PPR) signaling in osteocytes regulates anabolic and catabolic skeletal responses to PTH. *The Journal of biological chemistry*. 2013;288(28):20122-20134.

8. van Abel M, Hoenderop JG, van der Kemp AW, Friedlaender MM, van Leeuwen JP, Bindels RJ. Coordinated control of renal Ca(2+) transport proteins by parathyroid hormone. *Kidney international*. 2005;68(4):1708-1721.
9. de Groot T, Lee K, Langeslag M, Xi Q, Jalink K, Bindels RJ, Hoenderop JG. Parathyroid hormone activates TRPV5 via PKA-dependent phosphorylation. *Journal of the American Society of Nephrology : JASN*. 2009;20(8):1693-1704.
10. Biber J, Hernando N, Forster I, Murer H. Regulation of phosphate transport in proximal tubules. *Pflugers Archiv : European journal of physiology*. 2009;458(1):39-52.
11. Picard N, Capuano P, Stange G, Mihailova M, Kaissling B, Murer H, Biber J, Wagner CA. Acute parathyroid hormone differentially regulates renal brush border membrane phosphate cotransporters. *Pflugers Archiv : European journal of physiology*. 2010;460(3):677-687.
12. Nagai S, Okazaki M, Segawa H, Bergwitz C, Dean T, Potts JT, Jr., Mahon MJ, Gardella TJ, Juppner H. Acute down-regulation of sodium-dependent phosphate transporter NPT2a involves predominantly the cAMP/PKA pathway as revealed by signaling-selective parathyroid hormone analogs. *The Journal of biological chemistry*. 2011;286(2):1618-1626.
13. Suva LJ, Winslow GA, Wettenhall RE, Hammonds RG, Moseley JM, Diefenbach-Jagger H, Rodda CP, Kemp BE, Rodriguez H, Chen EY, et al. A parathyroid hormone-related protein implicated in malignant hypercalcemia: cloning and expression. *Science*. 1987;237(4817):893-896.
14. Nissenson RA, Diep D, Strewler GJ. Synthetic peptides comprising the amino-terminal sequence of a parathyroid hormone-like protein from human malignancies. Binding to parathyroid hormone receptors and activation of adenylate cyclase in bone cells and kidney. *The Journal of biological chemistry*. 1988;263(26):12866-12871.
15. McCauley LK, Martin TJ. Twenty-five years of PTHrP progress: from cancer hormone to multifunctional cytokine. *J Bone Miner Res*. 2012;27(6):1231-1239.
16. Karaplis AC, Luz A, Glowacki J, Bronson RT, Tybulewicz VL, Kronenberg HM, Mulligan RC. Lethal skeletal dysplasia from targeted disruption of the parathyroid hormone-related peptide gene. *Genes & development*. 1994;8(3):277-289.
17. Wysolmerski JJ, Stewart AF. The physiology of parathyroid hormone-related protein: an emerging role as a developmental factor. *Annual review of physiology*. 1998;60:431-460.
18. Philbrick WM, Dreyer BE, Nakchbandi IA, Karaplis AC. Parathyroid hormone-related protein is required for tooth eruption. *Proceedings of the National Academy of Sciences of the United States of America*. 1998;95(20):11846-11851.

19. Philbrick WM, Wysolmerski JJ, Galbraith S, Holt E, Orloff JJ, Yang KH, Vasavada RC, Weir EC, Broadus AE, Stewart AF. Defining the roles of parathyroid hormone-related protein in normal physiology. *Physiol Rev*. 1996;76(1):127-173.
20. Dean T, Vilardaga JP, Potts JT, Jr., Gardella TJ. Altered selectivity of parathyroid hormone (PTH) and PTH-related protein (PTHrP) for distinct conformations of the PTH/PTHrP receptor. *Mol Endocrinol*. 2008;22(1):156-166.
21. White AD, Fang F, Jean-Alphonse FG, Clark LJ, An HJ, Liu H, Zhao Y, Reynolds SL, Lee S, Xiao K, Sutkeviciute I, Vilardaga JP. Ca(2+) allostery in PTH-receptor signaling. *Proceedings of the National Academy of Sciences of the United States of America*. 2019;116(8):3294-3299.
22. Potts JT, Jr., Tregear GW, Keutmann HT, Niall HD, Sauer R, Deftos LJ, Dawson BF, Hogan ML, Aurbach GD. Synthesis of a biologically active N-terminal tetratriacontapeptide of parathyroid hormone. *Proceedings of the National Academy of Sciences of the United States of America*. 1971;68(1):63-67.
23. Cheloha RW, Gellman SH, Vilardaga JP, Gardella TJ. PTH receptor-1 signalling-mechanistic insights and therapeutic prospects. *Nat Rev Endocrinol*. 2015;11(12):712-724.
24. Jobert AS, Zhang P, Couvineau A, Bonaventure J, Roume J, Le Merrer M, Silve C. Absence of functional receptors for parathyroid hormone and parathyroid hormone-related peptide in Blomstrand chondrodysplasia. *J Clin Invest*. 1998;102(1):34-40.
25. Hoogendam J, Farih-Sips H, Wynaendts LC, Lowik CW, Wit JM, Karperien M. Novel mutations in the parathyroid hormone (PTH)/PTH-related peptide receptor type 1 causing Blomstrand osteochondrodysplasia types I and II. *J Clin Endocrinol Metab*. 2007;92(3):1088-1095.
26. Pansuriya TC, Kroon HM, Bovee JV. Enchondromatosis: insights on the different subtypes. *Int J Clin Exp Pathol*. 2010;3(6):557-569.
27. Hanisch M, Hanisch L, Kleinheinz J, Jung S. Primary failure of eruption (PFE): a systematic review. *Head Face Med*. 2018;14(1):5.
28. Tokavanich N, Gupta A, Nagata M, Takahashi A, Matsushita Y, Yatabe M, Ruellas A, Cevidanes L, Maki K, Yamaguchi T, Ono N, Ono W. A three-dimensional analysis of primary failure of eruption in humans and mice. *Oral Dis*. 2020;26(2):391-400.
29. Schipani E, Kruse K, Juppner H. A constitutively active mutant PTH-PTHrP receptor in Jansen-type metaphyseal chondrodysplasia. *Science*. 1995;268(5207):98-100.
30. Schipani E, Langman C, Hunzelman J, Le Merrer M, Loke KY, Dillon MJ, Silve C, Juppner H. A novel parathyroid hormone (PTH)/PTH-related peptide receptor mutation

in Jansen's metaphyseal chondrodysplasia. *J Clin Endocrinol Metab*. 1999;84(9):3052-3057.

31. Schipani E, Langman CB, Parfitt AM, Jensen GS, Kikuchi S, Kooh SW, Cole WG, Juppner H. Constitutively activated receptors for parathyroid hormone and parathyroid hormone-related peptide in Jansen's metaphyseal chondrodysplasia. *N Engl J Med*. 1996;335(10):708-714.
32. Feldenzer KL, Sarno J. Hypercalcemia of Malignancy. *J Adv Pract Oncol*. 2018;9(5):496-504.
33. Giovanella L, Bacigalupo L, Treglia G, Piccardo A. Will 18F-fluorocholine PET/CT replace other methods of preoperative parathyroid imaging? *Endocrine*. 2020.
34. Rubin MR. Recent advances in understanding and managing hypoparathyroidism. *F1000Res*. 2020;9.
35. Canalis E, Giustina A, Bilezikian JP. Mechanisms of anabolic therapies for osteoporosis. *N Engl J Med*. 2007;357(9):905-916.
36. Cohen A, Shiau S, Nair N, Recker RR, Lappe JM, Dempster DW, Nickolas TL, Zhou H, Agarwal S, Kamanda-Kosseh M, Bucovsky M, Williams JM, McMahon DJ, Stubby J, Shane E. Effect of Teriparatide on Bone Remodeling and Density in Premenopausal Idiopathic Osteoporosis: A Phase II Trial. *J Clin Endocrinol Metab*. 2020;105(10).
37. Ono K, Ohashi S, Oka H, Kadono Y, Yasui T, Matsumoto T, Omata Y, Tanaka S. Evaluations of daily teriparatide using finite-element analysis over 12 months in rheumatoid arthritis patients. *J Bone Miner Metab*. 2020.
38. Neer RM, Arnaud CD, Zanchetta JR, Prince R, Gaich GA, Reginster JY, Hodsman AB, Eriksen EF, Ish-Shalom S, Genant HK, Wang O, Mitlak BH. Effect of parathyroid hormone (1-34) on fractures and bone mineral density in postmenopausal women with osteoporosis. *N Engl J Med*. 2001;344(19):1434-1441.
39. Leder BZ, O'Dea LS, Zanchetta JR, Kumar P, Banks K, McKay K, Lyttle CR, Hattersley G. Effects of abaloparatide, a human parathyroid hormone-related peptide analog, on bone mineral density in postmenopausal women with osteoporosis. *J Clin Endocrinol Metab*. 2015;100(2):697-706.
40. Sleeman A, Clements JN. Abaloparatide: A new pharmacological option for osteoporosis. *American Journal of Health-System Pharmacy*. 2019;76(3):130-135.
41. Miller PD, Hattersley G, Lau E, Fitzpatrick LA, Harris AG, Williams GC, Hu MY, Riis BJ, Russo L, Christiansen C. Bone mineral density response rates are greater in patients treated with abaloparatide compared with those treated with placebo or teriparatide: Results from the ACTIVE phase 3 trial. *Bone*. 2019;120:137-140.

42. Arlt H, Mullarkey T, Hu D, Baron R, Ominsky MS, Mitlak B, Lanske B, Besschetnova T. Effects of abaloparatide and teriparatide on bone resorption and bone formation in female mice. *Bone Reports*. 2020;13:100291.
43. Hattersley G, Dean T, Corbin BA, Bahar H, Gardella TJ. Binding Selectivity of Abaloparatide for PTH-Type-1-Receptor Conformations and Effects on Downstream Signaling. *Endocrinology*. 2016;157(1):141-149.
44. Schiöth HB, Fredriksson R. The GRAFS classification system of G-protein coupled receptors in comparative perspective. *Gen Comp Endocrinol*. 2005;142(1-2):94-101.
45. Alexander SP, Davenport AP, Kelly E, Marrion N, Peters JA, Benson HE, Faccenda E, Pawson AJ, Sharman JL, Southan C, Davies JA, Collaborators C. The Concise Guide to PHARMACOLOGY 2015/16: G protein-coupled receptors. *Br J Pharmacol*. 2015;172(24):5744-5869.
46. Pándy-Szekeres G, Munk C, Tsonkov TM, Mordalski S, Harpsøe K, Hauser AS, Bojarski AJ, Gloriam DE. GPCRdb in 2018: adding GPCR structure models and ligands. *Nucleic Acids Research*. 2017;46(D1):D440-D446.
47. Congreve M, de Graaf C, Swain NA, Tate CG. Impact of GPCR Structures on Drug Discovery. *Cell*. 2020;181(1):81-91.
48. Pal K, Melcher K, Xu HE. Structure and mechanism for recognition of peptide hormones by Class B G-protein-coupled receptors. *Acta pharmacologica Sinica*. 2012;33(3):300-311.
49. Palczewski K, Kumasaka T, Hori T, Behnke CA, Motoshima H, Fox BA, Le Trong I, Teller DC, Okada T, Stenkamp RE, Yamamoto M, Miyano M. Crystal structure of rhodopsin: A G protein-coupled receptor. *Science*. 2000;289(5480):739-745.
50. de Graaf C, Song G, Cao C, Zhao Q, Wang MW, Wu B, Stevens RC. Extending the Structural View of Class B GPCRs. *Trends Biochem Sci*. 2017;42(12):946-960.
51. Lefkowitz RJ. Seven transmembrane receptors: something old, something new. *Acta Physiol (Oxf)*. 2007;190(1):9-19.
52. Lefkowitz RJ. Seven transmembrane receptors: a brief personal retrospective. *Biochim Biophys Acta*. 2007;1768(4):748-755.
53. Oldham WM, Hamm HE. Structural basis of function in heterotrimeric G proteins. *Q Rev Biophys*. 2006;39(2):117-166.
54. Neves SR, Ram PT, Iyengar R. G protein pathways. *Science*. 2002;296(5573):1636-1639.
55. Oldham WM, Hamm HE. Heterotrimeric G protein activation by G-protein-coupled receptors. *Nature Reviews Molecular Cell Biology*. 2008;9(1):60-71.

56. Rasmussen SG, DeVree BT, Zou Y, Kruse AC, Chung KY, Kobilka TS, Thian FS, Chae PS, Pardon E, Calinski D, Mathiesen JM, Shah ST, Lyons JA, Caffrey M, Gellman SH, Steyaert J, Skiniotis G, Weis WI, Sunahara RK, Kobilka BK. Crystal structure of the beta2 adrenergic receptor-Gs protein complex. *Nature*. 2011;477(7366):549-555.
57. Dupré DJ, Robitaille M, Rebois RV, Hébert TE. The Role of Gβγ Subunits in the Organization, Assembly, and Function of GPCR Signaling Complexes. *Annual Review of Pharmacology and Toxicology*. 2009;49(1):31-56.
58. Vadas O, Dbouk HA, Shymanets A, Perisic O, Burke JE, Abi Saab WF, Khalil BD, Harteneck C, Bresnick AR, Nurnberg B, Backer JM, Williams RL. Molecular determinants of PI3Kgamma-mediated activation downstream of G-protein-coupled receptors (GPCRs). *Proceedings of the National Academy of Sciences of the United States of America*. 2013;110(47):18862-18867.
59. Dicker F, Quitterer U, Winstel R, Honold K, Lohse MJ. Phosphorylation-independent inhibition of parathyroid hormone receptor signaling by G protein-coupled receptor kinases. *Proceedings of the National Academy of Sciences of the United States of America*. 1999;96(10):5476-5481.
60. Lohse MJ, Andexinger S, Pitcher J, Trukawinski S, Codina J, Faure JP, Caron MG, Lefkowitz RJ. Receptor-specific desensitization with purified proteins. Kinase dependence and receptor specificity of beta-arrestin and arrestin in the beta 2-adrenergic receptor and rhodopsin systems. *The Journal of biological chemistry*. 1992;267(12):8558-8564.
61. Drake MT, Shenoy SK, Lefkowitz RJ. Trafficking of G protein-coupled receptors. *Circ Res*. 2006;99(6):570-582.
62. Goodman OB, Jr., Krupnick JG, Santini F, Gurevich VV, Penn RB, Gagnon AW, Keen JH, Benovic JL. Beta-arrestin acts as a clathrin adaptor in endocytosis of the beta2-adrenergic receptor. *Nature*. 1996;383(6599):447-450.
63. Lin FT, Krueger KM, Kendall HE, Daaka Y, Fredericks ZL, Pitcher JA, Lefkowitz RJ. Clathrin-mediated endocytosis of the beta-adrenergic receptor is regulated by phosphorylation/dephosphorylation of beta-arrestin1. *The Journal of biological chemistry*. 1997;272(49):31051-31057.
64. Hamm HE. How activated receptors couple to G proteins. *Proceedings of the National Academy of Sciences of the United States of America*. 2001;98(9):4819-4821.
65. Krueger KM, Daaka Y, Pitcher JA, Lefkowitz RJ. The role of sequestration in G protein-coupled receptor resensitization. Regulation of beta2-adrenergic receptor dephosphorylation by vesicular acidification. *The Journal of biological chemistry*. 1997;272(1):5-8.

66. Abou-Samra AB, Juppner H, Force T, Freeman MW, Kong XF, Schipani E, Urena P, Richards J, Bonventre JV, Potts JT, Jr., et al. Expression cloning of a common receptor for parathyroid hormone and parathyroid hormone-related peptide from rat osteoblast-like cells: a single receptor stimulates intracellular accumulation of both cAMP and inositol trisphosphates and increases intracellular free calcium. *Proceedings of the National Academy of Sciences of the United States of America*. 1992;89(7):2732-2736.
67. Singh AT, Gilchrist A, Voyno-Yasenetskaya T, Radeff-Huang JM, Stern PH. G alpha12/G alpha13 subunits of heterotrimeric G proteins mediate parathyroid hormone activation of phospholipase D in UMR-106 osteoblastic cells. *Endocrinology*. 2005;146(5):2171-2175.
68. Singh AT, Frohman MA, Stern PH. Parathyroid hormone stimulates phosphatidylethanolamine hydrolysis by phospholipase D in osteoblastic cells. *Lipids*. 2005;40(11):1135-1140.
69. Avet C, Mancini A, Breton B, Le Gouill C, Hauser AS, Normand C, Kobayashi H, Gross F, Hogue M, Lukasheva V, St-Onge S, Carrier M, Heroux M, Morissette S, Fauman EB, Fortin JP, Schann S, Leroy X, Gloriam DE, Bouvier M. Effector membrane translocation biosensors reveal G protein and betaarrestin coupling profiles of 100 therapeutically relevant GPCRs. *Elife*. 2022;11.
70. Fraher LJ, Hodsman AB, Jonas K, Saunders D, Rose CI, Henderson JE, Hendy GN, Goltzman D. A comparison of the in vivo biochemical responses to exogenous parathyroid hormone-(1-34) [PTH-(1-34)] and PTH-related peptide-(1-34) in man. *J Clin Endocrinol Metab*. 1992;75(2):417-423.
71. Vilardaga JP, Gardella TJ, Wehbi VL, Feinstein TN. Non-canonical signaling of the PTH receptor. *Trends Pharmacol Sci*. 2012;33(8):423-431.
72. Malecz N, Bambino T, Bencsik M, Nissenson RA. Identification of phosphorylation sites in the G protein-coupled receptor for parathyroid hormone. Receptor phosphorylation is not required for agonist-induced internalization. *Mol Endocrinol*. 1998;12(12):1846-1856.
73. Castro M, Dicker F, Vilardaga JP, Krasel C, Bernhardt M, Lohse MJ. Dual regulation of the parathyroid hormone (PTH)/PTH-related peptide receptor signaling by protein kinase C and beta-arrestins. *Endocrinology*. 2002;143(10):3854-3865.
74. Vilardaga JP, Krasel C, Chauvin S, Bambino T, Lohse MJ, Nissenson RA. Internalization determinants of the parathyroid hormone receptor differentially regulate beta-arrestin/receptor association. *The Journal of biological chemistry*. 2002;277(10):8121-8129.

75. Mullershausen F, Zecri F, Cetin C, Billich A, Guerini D, Seuwen K. Persistent signaling induced by FTY720-phosphate is mediated by internalized S1P1 receptors. *Nature chemical biology*. 2009;5(6):428-434.
76. Ferrandon S, Feinstein TN, Castro M, Wang B, Bouley R, Potts JT, Gardella TJ, Vilardaga JP. Sustained cyclic AMP production by parathyroid hormone receptor endocytosis. *Nature chemical biology*. 2009;5(10):734-742.
77. Wehbi VL, Stevenson HP, Feinstein TN, Calero G, Romero G, Vilardaga JP. Noncanonical GPCR signaling arising from a PTH receptor-arrestin-Gbetagamma complex. *Proceedings of the National Academy of Sciences of the United States of America*. 2013;110(4):1530-1535.
78. Calebiro D, Nikolaev VO, Gagliani MC, de Filippis T, Dees C, Tacchetti C, Persani L, Lohse MJ. Persistent cAMP-signals triggered by internalized G-protein-coupled receptors. *PLoS Biol*. 2009;7(8):e1000172.
79. Feinstein TN, Yui N, Webber MJ, Wehbi VL, Stevenson HP, King JD, Jr., Hallows KR, Brown D, Bouley R, Vilardaga JP. Noncanonical control of vasopressin receptor type 2 signaling by retromer and arrestin. *The Journal of biological chemistry*. 2013;288(39):27849-27860.
80. Sutkeviciute I, Vilardaga JP. Structural insights into emergent signaling modes of G protein-coupled receptors. *The Journal of biological chemistry*. 2020;295(33):11626-11642.
81. Crilly SE, Puthenveedu MA. Compartmentalized GPCR Signaling from Intracellular Membranes. *J Membr Biol*. 2021;254(3):259-271.
82. Okazaki M, Ferrandon S, Vilardaga JP, Bouxsein ML, Potts JT, Jr., Gardella TJ. Prolonged signaling at the parathyroid hormone receptor by peptide ligands targeted to a specific receptor conformation. *Proceedings of the National Academy of Sciences of the United States of America*. 2008;105(43):16525-16530.
83. Maeda A, Okazaki M, Baron DM, Dean T, Khatri A, Mahon M, Segawa H, Abou-Samra AB, Juppner H, Bloch KD, Potts JT, Jr., Gardella TJ. Critical role of parathyroid hormone (PTH) receptor-1 phosphorylation in regulating acute responses to PTH. *Proceedings of the National Academy of Sciences of the United States of America*. 2013;110(15):5864-5869.
84. Pioszak AA, Xu HE. Molecular recognition of parathyroid hormone by its G protein-coupled receptor. *Proceedings of the National Academy of Sciences of the United States of America*. 2008;105(13):5034-5039.

85. Pioszak AA, Parker NR, Gardella TJ, Xu HE. Structural basis for parathyroid hormone-related protein binding to the parathyroid hormone receptor and design of conformation-selective peptides. *The Journal of biological chemistry*. 2009;284(41):28382-28391.
86. Goltzman D, Peytremann A, Callahan E, Tregear GW, Potts JT, Jr. Analysis of the requirements for parathyroid hormone action in renal membranes with the use of inhibiting analogues. *The Journal of biological chemistry*. 1975;250(8):3199-3203.
87. Zhao LH, Ma S, Sutkeviciute I, Shen DD, Zhou XE, de Waal PW, Li CY, Kang Y, Clark LJ, Jean-Alphonse FG, White AD, Yang D, Dai A, Cai X, Chen J, Li C, Jiang Y, Watanabe T, Gardella TJ, Melcher K, Wang MW, Vilardaga JP, Xu HE, Zhang Y. Structure and dynamics of the active human parathyroid hormone receptor-1. *Science*. 2019;364(6436):148-153.
88. Horiuchi N, Holick MF, Potts JT, Jr., Rosenblatt M. A parathyroid hormone inhibitor in vivo: design and biological evaluation of a hormone analog. *Science*. 1983;220(4601):1053-1055.
89. Shimizu M, Carter PH, Gardella TJ. Autoactivation of type-1 parathyroid hormone receptors containing a tethered ligand. *The Journal of biological chemistry*. 2000;275(26):19456-19460.
90. Shimizu M, Potts JT, Jr., Gardella TJ. Minimization of parathyroid hormone. Novel amino-terminal parathyroid hormone fragments with enhanced potency in activating the type-1 parathyroid hormone receptor. *The Journal of biological chemistry*. 2000;275(29):21836-21843.
91. Shimizu N, Guo J, Gardella TJ. Parathyroid hormone (PTH)-(1-14) and -(1-11) analogs conformationally constrained by alpha-aminoisobutyric acid mediate full agonist responses via the juxtamembrane region of the PTH-1 receptor. *The Journal of biological chemistry*. 2001;276(52):49003-49012.
92. Shimizu M, Carter PH, Khatri A, Potts JT, Jr., Gardella TJ. Enhanced activity in parathyroid hormone-(1-14) and -(1-11): novel peptides for probing ligand-receptor interactions. *Endocrinology*. 2001;142(7):3068-3074.
93. Noda H, Okazaki M, Joyashiki E, Tamura T, Kawabe Y, Khatri A, Jueppner H, Potts JT, Jr., Gardella TJ, Shimizu M. Optimization of PTH/PTHrP Hybrid Peptides to Derive a Long-Acting PTH Analog (LA-PTH). *JBMR Plus*. 2020;4(7):e10367.
94. Jean-Alphonse FG, Wehbi VL, Chen J, Noda M, Taboas JM, Xiao K, Vilardaga JP. beta2-adrenergic receptor control of endosomal PTH receptor signaling via Gbetagamma. *Nature chemical biology*. 2017;13(3):259-261.
95. Shimizu M, Joyashiki E, Noda H, Watanabe T, Okazaki M, Nagayasu M, Adachi K, Tamura T, Potts JT, Jr., Gardella TJ, Kawabe Y. Pharmacodynamic Actions of a Long-

Acting PTH Analog (LA-PTH) in Thyroparathyroidectomized (TPTX) Rats and Normal Monkeys. *J Bone Miner Res*. 2016;31(7):1405-1412.

96. Feinstein TN, Wehbi VL, Ardura JA, Wheeler DS, Ferrandon S, Gardella TJ, Vilardaga JP. Retromer terminates the generation of cAMP by internalized PTH receptors. *Nature chemical biology*. 2011;7(5):278-284.

97. White AD, Jean-Alphonse FG, Fang F, Pena KA, Liu S, Konig GM, Inoue A, Aslanoglou D, Gellman SH, Kostenis E, Xiao K, Vilardaga JP. Gq/11-dependent regulation of endosomal cAMP generation by parathyroid hormone class B GPCR. *Proceedings of the National Academy of Sciences of the United States of America*. 2020;117(13):7455-7460.

98. Collins BM, Norwood SJ, Kerr MC, Mahony D, Seaman MN, Teasdale RD, Owen DJ. Structure of Vps26B and mapping of its interaction with the retromer protein complex. *Traffic (Copenhagen, Denmark)*. 2008;9(3):366-379.

99. Bonifacino JS, Rojas R. Retrograde transport from endosomes to the trans-Golgi network. *Nature reviews Molecular cell biology*. 2006;7(8):568-579.

100. Gidon A, Al-Bataineh MM, Jean-Alphonse FG, Stevenson HP, Watanabe T, Louet C, Khatri A, Calero G, Pastor-Soler NM, Gardella TJ, Vilardaga JP. Endosomal GPCR signaling turned off by negative feedback actions of PKA and v-ATPase. *Nature chemical biology*. 2014;10(9):707-709.

101. Pioszak AA, Harikumar KG, Parker NR, Miller LJ, Xu HE. Dimeric arrangement of the parathyroid hormone receptor and a structural mechanism for ligand-induced dissociation. *The Journal of biological chemistry*. 2010;285(16):12435-12444.

102. Ehrenmann J, Schoppe J, Klenk C, Rappas M, Kummer L, Dore AS, Pluckthun A. High-resolution crystal structure of parathyroid hormone 1 receptor in complex with a peptide agonist. *Nat Struct Mol Biol*. 2018;25(12):1086-1092.

103. Ma S, Shen Q, Zhao LH, Mao C, Zhou XE, Shen DD, de Waal PW, Bi P, Li C, Jiang Y, Wang MW, Sexton PM, Wootten D, Melcher K, Zhang Y, Xu HE. Molecular Basis for Hormone Recognition and Activation of Corticotropin-Releasing Factor Receptors. *Mol Cell*. 2020;77(3):669-680.e664.

104. Qiao A, Han S, Li X, Li Z, Zhao P, Dai A, Chang R, Tai L, Tan Q, Chu X, Ma L, Thorsen TS, Reedtz-Runge S, Yang D, Wang MW, Sexton PM, Wootten D, Sun F, Zhao Q, Wu B. Structural basis of Gs and Gi recognition by the human glucagon receptor. *Science*. 2020;367(6484):1346-1352.

105. Kobayashi K, Shihoya W, Nishizawa T, Kadji FMN, Aoki J, Inoue A, Nureki O. Cryo-EM structure of the human PAC1 receptor coupled to an engineered heterotrimeric G protein. *Nat Struct Mol Biol*. 2020;27(3):274-280.

106. Liang YL, Belousoff MJ, Zhao P, Koole C, Fletcher MM, Truong TT, Julita V, Christopoulos G, Xu HE, Zhang Y, Khoshouei M, Christopoulos A, Danev R, Sexton PM, Wootten D. Toward a Structural Understanding of Class B GPCR Peptide Binding and Activation. *Mol Cell*. 2020;77(3):656-668.e655.
107. dal Maso E, Glukhova A, Zhu Y, Garcia-Nafria J, Tate CG, Atanasio S, Reynolds CA, Ramírez-Aportela E, Carazo J-M, Hick CA, Furness SGB, Hay DL, Liang Y-L, Miller LJ, Christopoulos A, Wang M-W, Wootten D, Sexton PM. The Molecular Control of Calcitonin Receptor Signaling. *ACS Pharmacology & Translational Science*. 2019;2(1):31-51.
108. Liang YL, Khoshouei M, Deganutti G, Glukhova A, Koole C, Peat TS, Radjainia M, Plitzko JM, Baumeister W, Miller LJ, Hay DL, Christopoulos A, Reynolds CA, Wootten D, Sexton PM. Cryo-EM structure of the active, Gs-protein complexed, human CGRP receptor. *Nature*. 2018;561(7724):492-497.
109. Liang YL, Khoshouei M, Glukhova A, Furness SGB, Zhao P, Clydesdale L, Koole C, Truong TT, Thal DM, Lei S, Radjainia M, Danev R, Baumeister W, Wang MW, Miller LJ, Christopoulos A, Sexton PM, Wootten D. Phase-plate cryo-EM structure of a biased agonist-bound human GLP-1 receptor-Gs complex. *Nature*. 2018;555(7694):121-125.
110. Zhang Y, Sun B, Feng D, Hu H, Chu M, Qu Q, Tarrasch JT, Li S, Sun Kobilka T, Kobilka BK, Skiniotis G. Cryo-EM structure of the activated GLP-1 receptor in complex with a G protein. *Nature*. 2017;546(7657):248-253.
111. Song G, Yang D, Wang Y, de Graaf C, Zhou Q, Jiang S, Liu K, Cai X, Dai A, Lin G, Liu D, Wu F, Wu Y, Zhao S, Ye L, Han GW, Lau J, Wu B, Hanson MA, Liu ZJ, Wang MW, Stevens RC. Human GLP-1 receptor transmembrane domain structure in complex with allosteric modulators. *Nature*. 2017;546(7657):312-315.
112. Hilger D, Kumar KK, Hu H, Pedersen MF, O'Brien ES, Giehm L, Jennings C, Eskici G, Inoue A, Lerch M, Mathiesen JM, Skiniotis G, Kobilka BK. Structural insights into differences in G protein activation by family A and family B GPCRs. *Science*. 2020;369(6503).
113. Dong M, Deganutti G, Piper SJ, Liang YL, Khoshouei M, Belousoff MJ, Harikumar KG, Reynolds CA, Glukhova A, Furness SGB, Christopoulos A, Danev R, Wootten D, Sexton PM, Miller LJ. Structure and dynamics of the active Gs-coupled human secretin receptor. *Nat Commun*. 2020;11(1):4137.
114. Duan J, Shen DD, Zhou XE, Bi P, Liu QF, Tan YX, Zhuang YW, Zhang HB, Xu PY, Huang SJ, Ma SS, He XH, Melcher K, Zhang Y, Xu HE, Jiang Y. Cryo-EM structure of an activated VIP1 receptor-G protein complex revealed by a NanoBiT tethering strategy. *Nat Commun*. 2020;11(1):4121.

115. Sun W, Chen LN, Zhou Q, Zhao LH, Yang D, Zhang H, Cong Z, Shen DD, Zhao F, Zhou F, Cai X, Chen Y, Zhou Y, Gadgaard S, van der Velden WJC, Zhao S, Jiang Y, Rosenkilde MM, Xu HE, Zhang Y, Wang MW. A unique hormonal recognition feature of the human glucagon-like peptide-2 receptor. *Cell Res*. 2020;30(12):1098-1108.
116. Zhao F, Zhang C, Zhou Q, Hang K, Zou X, Chen Y, Wu F, Rao Q, Dai A, Yin W, Shen DD, Zhang Y, Xia T, Stevens RC, Xu HE, Yang D, Zhao L, Wang MW. Structural insights into hormone recognition by the human glucose-dependent insulinotropic polypeptide receptor. *Elife*. 2021;10.
117. Wang X, Cheng X, Zhao L, Wang Y, Ye C, Zou X, Dai A, Cong Z, Chen J, Zhou Q, Xia T, Jiang H, Xu HE, Yang D, Wang MW. Molecular insights into differentiated ligand recognition of the human parathyroid hormone receptor 2. *Proceedings of the National Academy of Sciences of the United States of America*. 2021;118(32).
118. Josephs TM, Belousoff MJ, Liang YL, Piper SJ, Cao J, Garama DJ, Leach K, Gregory KJ, Christopoulos A, Hay DL, Danev R, Wootten D, Sexton PM. Structure and dynamics of the CGRP receptor in apo and peptide-bound forms. *Science*. 2021;372(6538).
119. Castro M, Nikolaev VO, Palm D, Lohse MJ, Vilardaga JP. Turn-on switch in parathyroid hormone receptor by a two-step parathyroid hormone binding mechanism. *Proceedings of the National Academy of Sciences of the United States of America*. 2005;102(44):16084-16089.
120. Clark LJ, Krieger J, White AD, Bondarenko V, Lei S, Fang F, Lee JY, Doruker P, Bottke T, Jean-Alphonse F, Tang P, Gardella TJ, Xiao K, Sutkeviciute I, Coin I, Bahar I, Vilardaga JP. Allosteric interactions in the parathyroid hormone GPCR-arrestin complex formation. *Nature chemical biology*. 2020;16(10):1096-1104.
121. Bahar I, Lezon TR, Bakan A, Shrivastava IH. Normal mode analysis of biomolecular structures: functional mechanisms of membrane proteins. *Chem Rev*. 2010;110(3):1463-1497.
122. Zhang Y, Doruker P, Kaynak B, Zhang S, Krieger J, Li H, Bahar I. Intrinsic dynamics is evolutionarily optimized to enable allosteric behavior. *Curr Opin Struct Biol*. 2020;62:14-21.
123. Lezon TR, Bahar I. Constraints imposed by the membrane selectively guide the alternating access dynamics of the glutamate transporter GltPh. *Biophys J*. 2012;102(6):1331-1340.
124. Li H, Chang YY, Lee JY, Bahar I, Yang LW. DynOmics: dynamics of structural proteome and beyond. *Nucleic Acids Res*. 2017;45(W1):W374-W380.

125. Kaynak BT, Bahar I, Doruker P. Essential site scanning analysis: A new approach for detecting sites that modulate the dispersion of protein global motions. *Comput Struct Biotechnol J*. 2020;18:1577-1586.
126. Sutkeviciute I, Lee JY, White AD, Maria CS, Pena KA, Savransky S, Doruker P, Li H, Lei S, Kaynak B, Tu C, Clark LJ, Sanker S, Gardella TJ, Chang W, Bahar I, Vilardaga JP. Precise druggability of the PTH type 1 receptor. *Nature chemical biology*. 2022;18(3):272-280.
127. Bueno AB, Sun B, Willard FS, Feng D, Ho JD, Wainscott DB, Showalter AD, Vieth M, Chen Q, Stutsman C, Chau B, Ficorilli J, Agejas FJ, Cumming GR, Jimenez A, Rojo I, Kobilka TS, Kobilka BK, Sloop KW. Structural insights into probe-dependent positive allosterism of the GLP-1 receptor. *Nature chemical biology*. 2020;16(10):1105-1110.
128. Tamura T, Noda H, Joyashiki E, Hoshino M, Watanabe T, Kinosaki M, Nishimura Y, Esaki T, Ogawa K, Miyake T, Arai S, Shimizu M, Kitamura H, Sato H, Kawabe Y. Identification of an orally active small-molecule PTHR1 agonist for the treatment of hypoparathyroidism. *Nat Commun*. 2016;7:13384.
129. Nishimura Y, Esaki T, Isshiki Y, Furuta Y, Mizutani A, Kotake T, Emura T, Watanabe Y, Ohta M, Nakagawa T, Ogawa K, Arai S, Noda H, Kitamura H, Shimizu M, Tamura T, Sato H. Lead Optimization and Avoidance of Reactive Metabolite Leading to PCO371, a Potent, Selective, and Orally Available Human Parathyroid Hormone Receptor 1 (hPTHR1) Agonist. *J Med Chem*. 2020;63(10):5089-5099.
130. Lee S, Mannstadt M, Guo J, Kim SM, Yi HS, Khatri A, Dean T, Okazaki M, Gardella TJ, Juppner H. A Homozygous [Cys25]PTH(1-84) Mutation That Impairs PTH/PTHrP Receptor Activation Defines a Novel Form of Hypoparathyroidism. *J Bone Miner Res*. 2015;30(10):1803-1813.
131. White A.D KAP, Lisa J. Clark, Christian Santa Maria4 Shi Liu, Frédéric G. Jean-Alphonse, Ji Young Lee, Saifei Lei, Zhiqiang Cheng, , Chia-Ling Tu, Fei Fang, Nicholas Szeto, Thomas J. Gardella, Kunhong Xiao, Samuel H. Gellman, Ivet Bahar, Ieva Sutkeviciute, Wenhan Chang, and Jean-Pierre Vilardaga. Decoding location bias information of cAMP signaling in a class B GPCR. *Science Signaling*. 2021(in Press).
132. Shukla AK, Manglik A, Kruse AC, Xiao K, Reis RI, Tseng WC, Staus DP, Hilger D, Uysal S, Huang LY, Paduch M, Tripathi-Shukla P, Koide A, Koide S, Weis WI, Kossiakoff AA, Kobilka BK, Lefkowitz RJ. Structure of active beta-arrestin-1 bound to a G-protein-coupled receptor phosphopeptide. *Nature*. 2013;497(7447):137-141.
133. Chen Q, Iverson TM, Gurevich VV. Structural Basis of Arrestin-Dependent Signal Transduction. *Trends Biochem Sci*. 2018;43(6):412-423.

134. Han M, Gurevich VV, Vishnivetskiy SA, Sigler PB, Schubert C. Crystal structure of beta-arrestin at 1.9 A: possible mechanism of receptor binding and membrane Translocation. *Structure*. 2001;9(9):869-880.
135. Zhou XE, He Y, de Waal PW, Gao X, Kang Y, Van Eps N, Yin Y, Pal K, Goswami D, White TA, Barty A, Latorraca NR, Chapman HN, Hubbell WL, Dror RO, Stevens RC, Cherezov V, Gurevich VV, Griffin PR, Ernst OP, Melcher K, Xu HE. Identification of Phosphorylation Codes for Arrestin Recruitment by G Protein-Coupled Receptors. *Cell*. 2017;170(3):457-469 e413.
136. Eichel K, Jullie D, Barsi-Rhyne B, Latorraca NR, Masureel M, Sibarita JB, Dror RO, von Zastrow M. Catalytic activation of beta-arrestin by GPCRs. *Nature*. 2018;557(7705):381-386.
137. Latorraca NR, Wang JK, Bauer B, Townshend RJL, Hollingsworth SA, Olivieri JE, Xu HE, Sommer ME, Dror RO. Molecular mechanism of GPCR-mediated arrestin activation. *Nature*. 2018;557(7705):452-456.
138. Laporte SA, Miller WE, Kim KM, Caron MG. beta-Arrestin/AP-2 interaction in G protein-coupled receptor internalization: identification of a beta-arrestin binging site in beta 2-adaptin. *The Journal of biological chemistry*. 2002;277(11):9247-9254.
139. Farrell IS, Toroney R, Hazen JL, Mehl RA, Chin JW. Photo-cross-linking interacting proteins with a genetically encoded benzophenone. *Nat Methods*. 2005;2(5):377-384.
140. Kang Y, Zhou XE, Gao X, He Y, Liu W, Ishchenko A, Barty A, White TA, Yefanov O, Han GW, Xu Q, de Waal PW, Ke J, Tan MH, Zhang C, Moeller A, West GM, Pascal BD, Van Eps N, Caro LN, Vishnivetskiy SA, Lee RJ, Suino-Powell KM, Gu X, Pal K, Ma J, Zhi X, Boutet S, Williams GJ, Messerschmidt M, Gati C, Zatsepin NA, Wang D, James D, Basu S, Roy-Chowdhury S, Conrad CE, Coe J, Liu H, Lisova S, Kupitz C, Grotjohann I, Fromme R, Jiang Y, Tan M, Yang H, Li J, Wang M, Zheng Z, Li D, Howe N, Zhao Y, Standfuss J, Diederichs K, Dong Y, Potter CS, Carragher B, Caffrey M, Jiang H, Chapman HN, Spence JC, Fromme P, Weierstall U, Ernst OP, Katritch V, Gurevich VV, Griffin PR, Hubbell WL, Stevens RC, Cherezov V, Melcher K, Xu HE. Crystal structure of rhodopsin bound to arrestin by femtosecond X-ray laser. *Nature*. 2015;523(7562):561-567.
141. Staus DP, Hu H, Robertson MJ, Kleinhenz ALW, Wingler LM, Capel WD, Latorraca NR, Lefkowitz RJ, Skiniotis G. Structure of the M2 muscarinic receptor-beta-arrestin complex in a lipid nanodisc. *Nature*. 2020.
142. Huang W, Masureel M, Qu Q, Janetzko J, Inoue A, Kato HE, Robertson MJ, Nguyen KC, Glenn JS, Skiniotis G, Kobilka BK. Structure of the neurotensin receptor 1 in complex with beta-arrestin 1. *Nature*. 2020.

143. Yin W, Li Z, Jin M, Yin YL, de Waal PW, Pal K, Yin Y, Gao X, He Y, Gao J, Wang X, Zhang Y, Zhou H, Melcher K, Jiang Y, Cong Y, Edward Zhou X, Yu X, Eric Xu H. A complex structure of arrestin-2 bound to a G protein-coupled receptor. *Cell Res*. 2019;29(12):971-983.
144. Shiraishi Y, Natsume M, Kofuku Y, Imai S, Nakata K, Mizukoshi T, Ueda T, Iwaï H, Shimada I. Phosphorylation-induced conformation of β(2)-adrenoceptor related to arrestin recruitment revealed by NMR. *Nat Commun*. 2018;9(1):194-194.
145. Ho PWM, Chan AS, Pavlos NJ, Sims NA, Martin TJ. Brief exposure to full length parathyroid hormone-related protein (PTHrP) causes persistent generation of cyclic AMP through an endocytosis-dependent mechanism. *Biochem Pharmacol*. 2019;169:113627.
146. Pena KA, White AD, Savransky S, Castillo IP, Jean-Alphonse FG, Gardella TJ, Sutkeviciute I, Vilardaga JP. Biased GPCR signaling by the native parathyroid hormone-related protein 1 to 141 relative to its N-terminal fragment 1 to 36. *The Journal of biological chemistry*. 2022;298(9):102332.

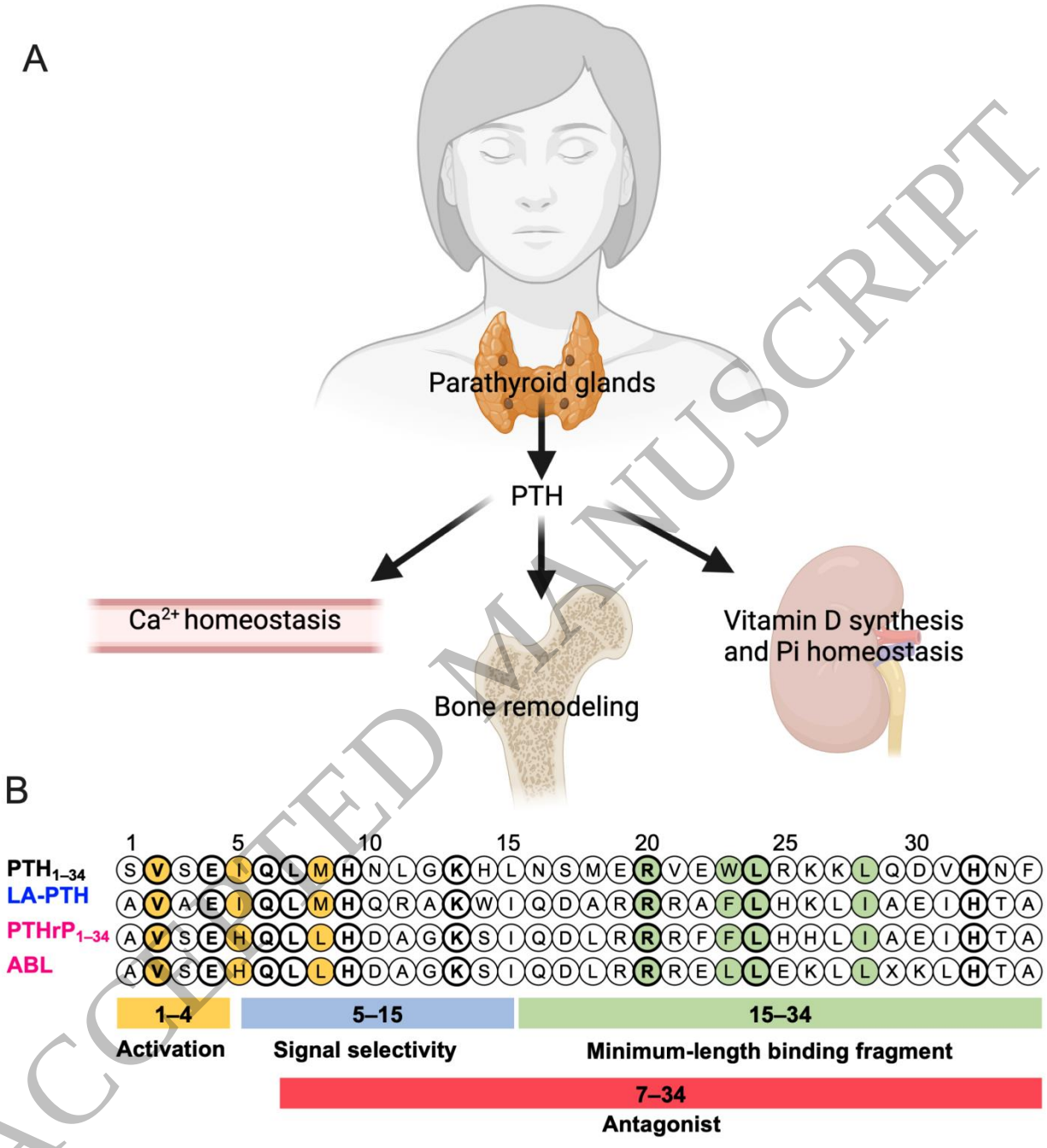

Figure 1. Functions and sequence of PTH. (**A**) Main PTH functions in the body. (**B**) Sequence alignment of PTH_1R peptide ligands. Residues conserved amongst all the listed PTH_1R peptide ligands are in bold. Residues critical for receptor activation are yellow orange, and residues critical for receptor binding are green. X is α-methylalanine in ABL.

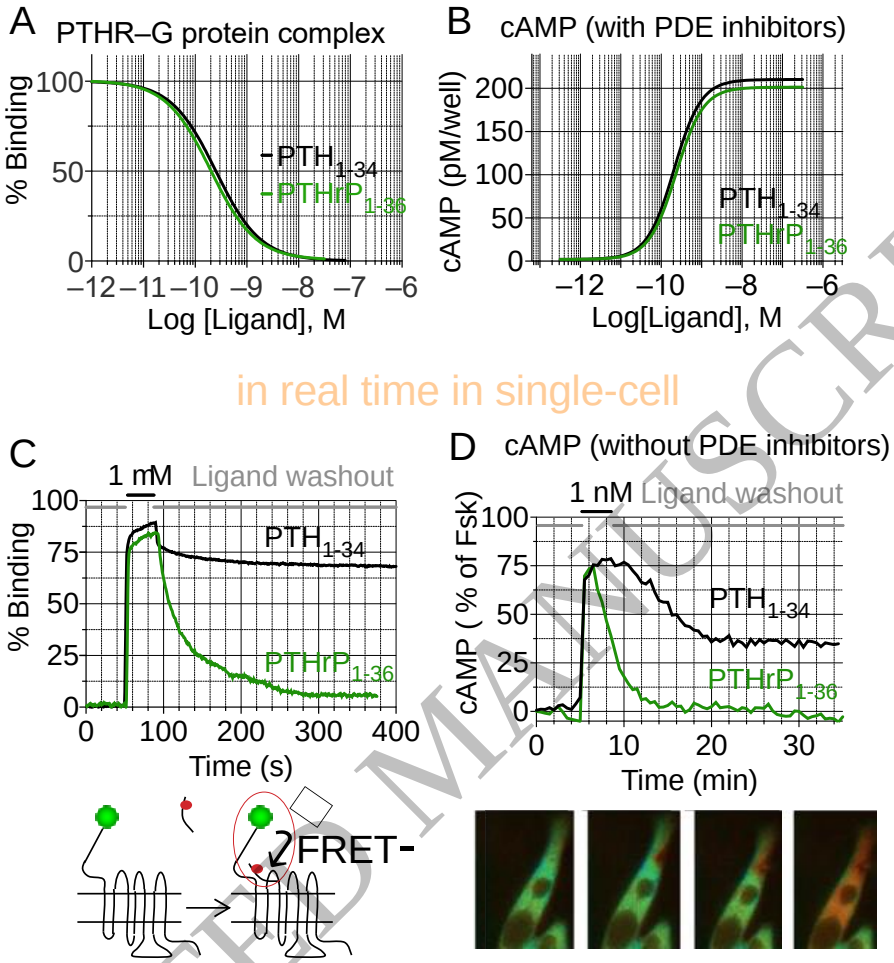

Figure 2. Pharmacological properties of PTH_1R. (**A**, **B**) Comparison between the competitive binding isotherms (A) and concentration-effect curves for cAMP accumulation in HEK293 cells expressing the recombinant human PTH_1R**.** (**C**) Recording real time binding of peptide ligands to PTH_1R in a single cell. Ligand and receptor interaction is measured by FRET between GFP-tagged PTH_1R and tetramethylrhodamine (TMR)-labeled peptide ligands. Shown are the changes of GFP emission due to a FRET increase in response to rapid superfusion of ligand-TMR (horizontal black bar). (**D**) cAMP production over 35 min measured by FRET changes from a single HEK293 cells stably expressing PTH_1R and transiently expressing the cytoplasmic cAMP FRET sensor epac1-CFP/YFP and in the absence of phosphodiesterase (PDE) inhibitors. Cells were continuously perfused with control buffer or peptide ligands (horizontal black bar)**.** Images show the propagation of the cAMP production represented as pseudocolored FRET ratio before (green) and after (red) stimulation of a single cell with $PTH_{1–34}$.

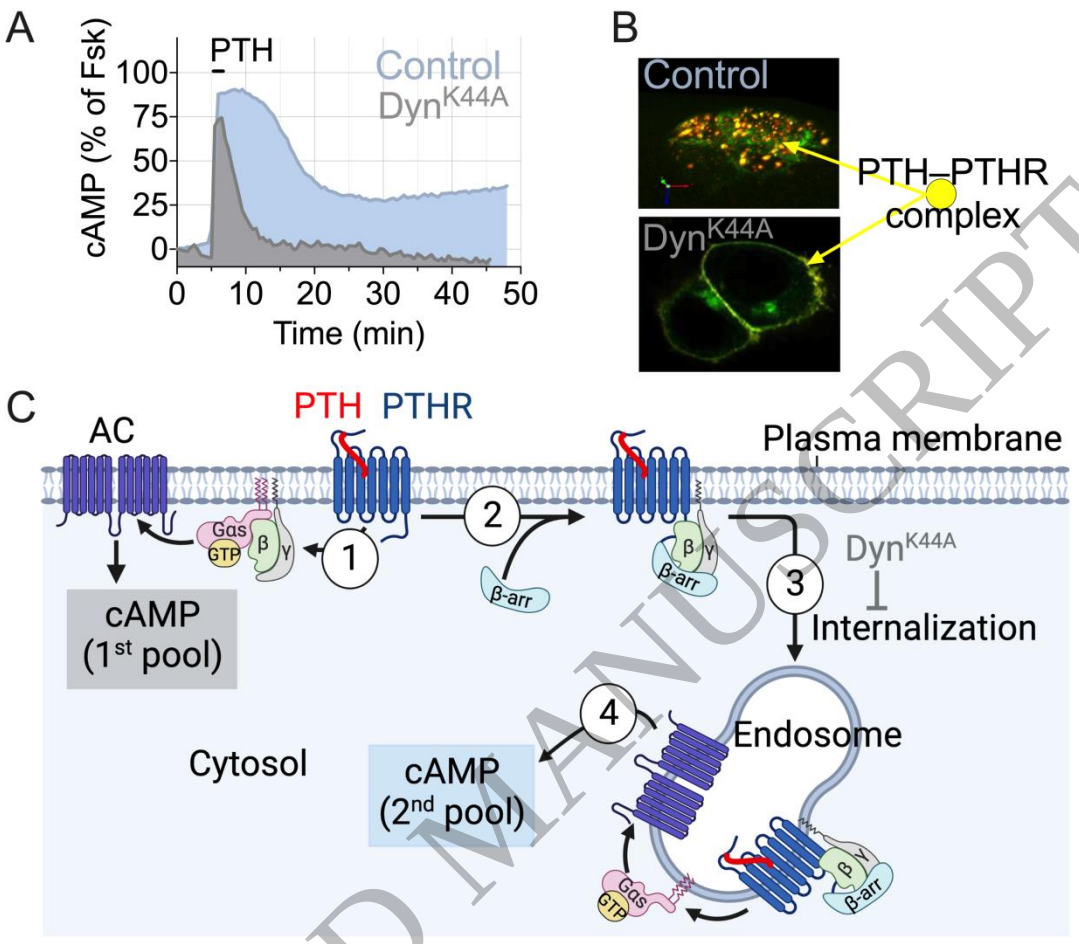

Figure 3. Modes of PTH_1R signaling via cAMP. (**A**) Time-courses of cAMP production induced by PTH_{1-34} in single cell (here a mouse osteoblast) without (control blue) or with (grey) expression of the recombinant dominant-negative dynamin mutant (DynK44A) that blocks receptor internalization. (**B**) Confocal Images representing a 3D view of HEK-293 cells expressing PTH_1R N-terminally tagged with GFP ($PTHR^{GFP}$, green) with TMR-labelled PTH_{1-34} (PTH^{TMR}, red). In control cells, PTH_1R^{GFP} and PTH^{TMR} colocalized (yellow spots) in endosomes; in cells coexpressing Dyn-K44A, the ligand–receptor complex remains at the cell surface. (**C**) The 1st pool of cAMP production takes place at the cell membrane following PTH binding to PTH_1R (step 1). This response is short-lived due to rapid receptor desensitization via PTHR phosphorylation by GPCR kinases, followed by recruitment of β-arrestins (βarrs) (step 2) driving receptor internalization and its redistribution in early endosomes (step 3). PTH interacts tightly with PTH_1R in a conformation-dependent fashion and induces the 2nd pool cAMP production from endosomes (step 4). Endosomal cAMP production is prolonged until endosomal acidification induces the release of PTH from the receptor. Created with BioRender.

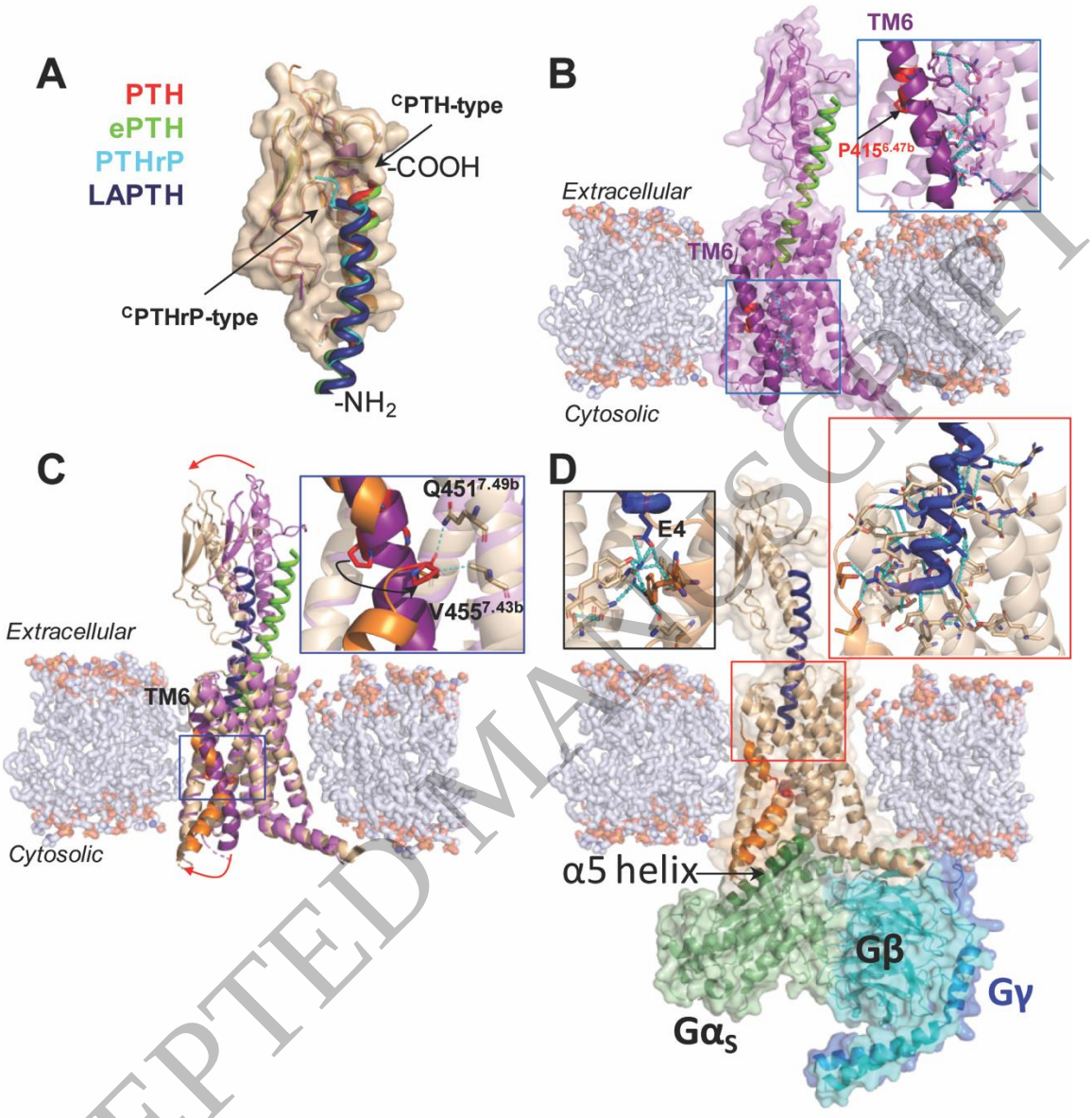

Figure 4. Structural characterization of PTH_1R activation. (A) Overlaid structures of PTH_1R^{ECD} in complex with distinct peptides, aligned by PTH_1R^{ECD}. PTH, *red coil* (PDB 3C4M); PTHrP, *cyan coil*, (PDB 3H3G); ePTH, *green coil* (PDB 6FJ3); LAPTH, *dark blue coil* (PDB 6NBF). The N- and C-termini of the peptides are denoted by $–NH_2$ and –COOH, respectively. (B) Crystal structure of inactive state PTHR bound to ePTH (*green coil*, PDB 6FJ3). (C) Overlay of inactive (receptor in purple, ePTH in *green*, PDB 6FJ3) and fully activated (receptor in wheat, LAPTH in dark blue, PDB 6NBF) PTH_1R structures, aligned by their TMDs. TM6 is in *deep purple* or *orange* in inactive and fully active states, respectively. (D) Cryo-EM structure of fully activated LAPTH-bound (*dark blue coil)* PTH_1R (state 1) coupled to G_s heterotrimer (PDB 6NBF).

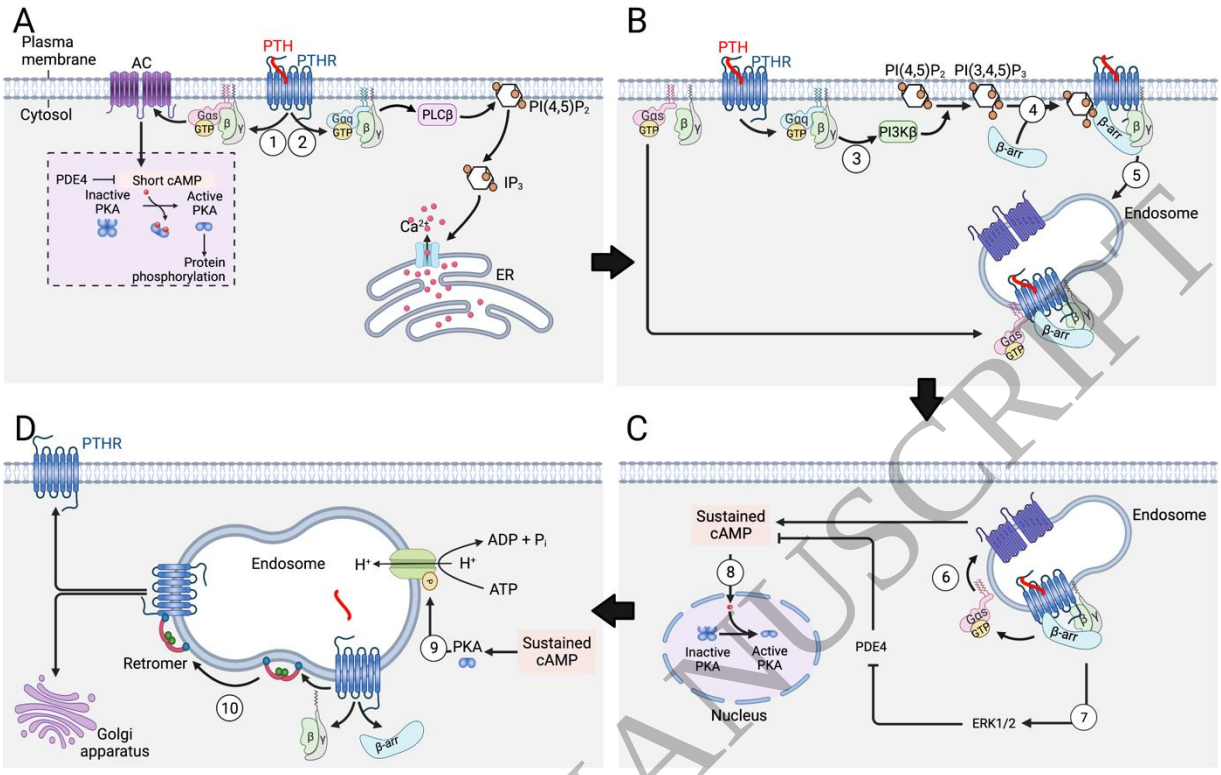

Figure 5. Mechanism of endosomal PTH_1R signaling via cAMP. (**A**) PTH_1R activates heterotrimeric G_s and G_q proteins at the plasma membrane in response to PTH (Steps 1 and 2). G_s activates adenylate cyclases (AC) leading to cAMP production and activation of cytosolic protein kinase A (PKA). The 1st pool of cAMP production is short due to the action of phosphodiesterases (PDE). G_q activates phospholipase C (PLC_β) that cleaves phosphatidylinositol (4,5)-bisphosphate ($PI(4,5)P_2$) into inositol (1,4,5)-trisphosphate (IP3). Free diffusing IP3 binds and activates IP3-gated Ca^{2+} channels, which in turn release stored Ca^{2+} into the cytosol. (**B**) Following Gq activation, Gβγ promotes PI3Kβ-dependent generation of $PI(3,4,5)P_3$ (step 3) at the plasma membrane that triggers β-arrestin (βarr) recruitment to the PTHR (step 4) and the formation and internalization of the ternary PTH_1R–βarr–Gβγ complex. Reassembly of the ternary PTH_1R complex with $G\alpha_s$ is thought to be dependent on $G\alpha_S$ diffusion.

(**C**) PTH triggers sustained cAMP production after receptor internalization to endosomes via a β-arrestins (βarr) and clathrin-coated-pit dependent pathway (2nd pool) (step 6). The sustained phase of endosomal cAMP production is due to the inhibitory action of extracellular signal-regulated protein kinase 1/2 (ERK1/2) on PDE4 (step 7). Endosome-generated cAMP can efficiently diffuse into the nucleus to activate nuclear PKA (step 8). (**D**) Endosomal cAMP production is prolonged until endosomal acidification caused by v-ATPase activity induces the release of PTH from the receptor (step 9) and assembly of the PTH_1R-retromer complex (step

10) allowing receptor transfer to the Golgi apparatus and receptor recycling. (Created with BioRender after adaptation from Sutkeviciute and Vilardaga (80).

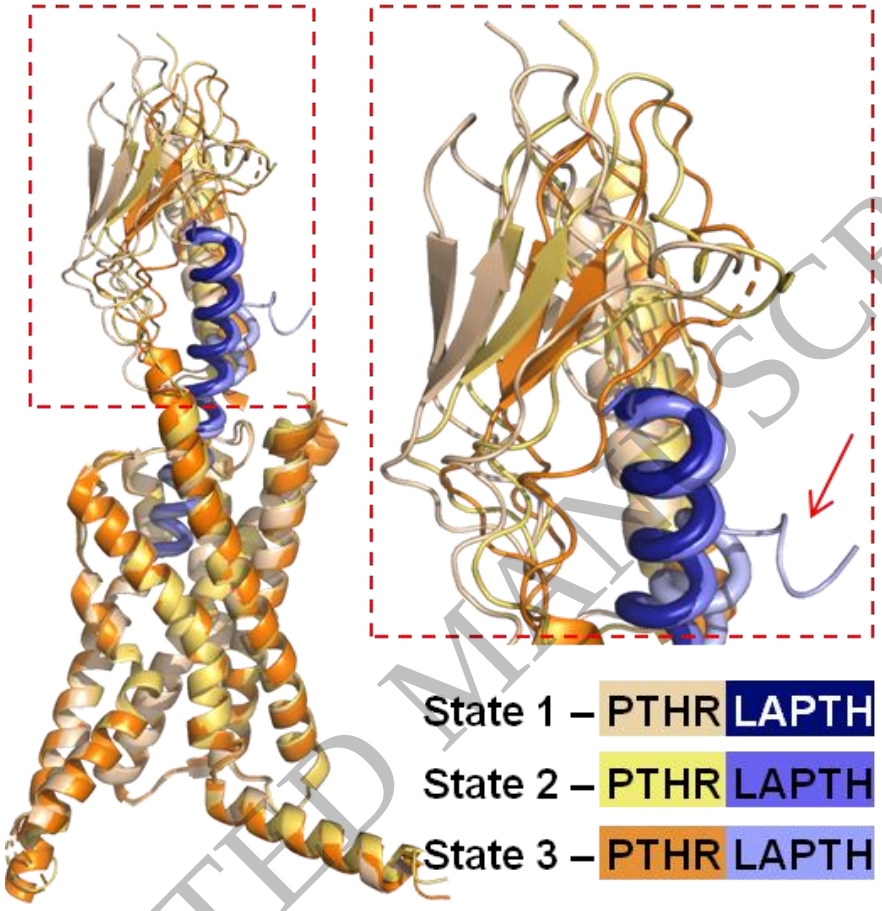

Figure 6. Structural dynamics of LA-PTH–PTH$_1$R complex. Overlaid three distinct conformational states of LA-PTH–PTH$_1$R complex obtained from cryo-EM data analysis, aligned by TMDs. PTH$_1$R and LA-PTH are shown as different shades of *purple* and *orange*, respectively. The oscillation of the PTH$_1$R^{ECD} is evident (close-up view), while the TMD core shows higher degree of stability, likely due to tight binding of ^{N}LA-PTH. Notably, state 3 captures the event of partial dissociation of ^{C}LA-PTH from PTH$_1$R^{ECD} (*red arrow*).

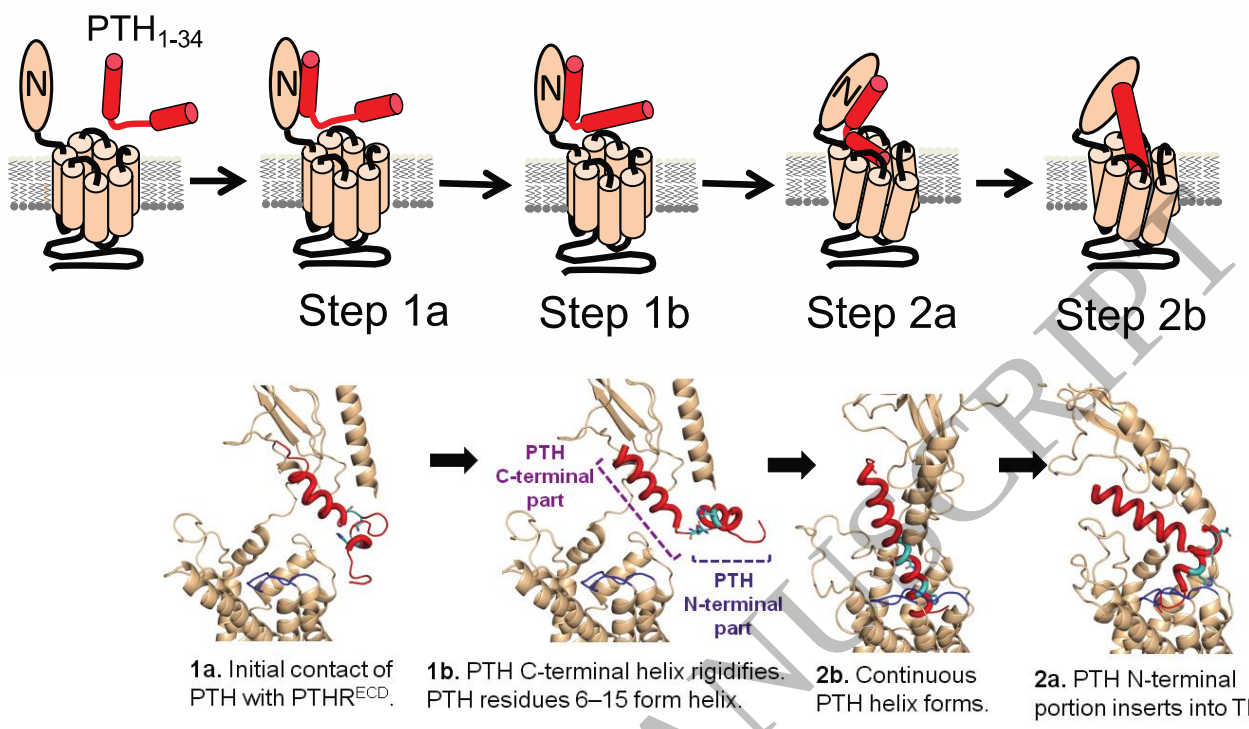

Figure 7. Expanded two-step model of PTH binding to PTH_1R. Schematic representation and structural model where PTH_1R is colored *wheat*, with ECL2 highlighted in *dark blue*. PTH is colored *red*, with residues His9, Asn16, and Ser17 displayed as *cyan* sticks. In the fast first step (Step 1), binding of the C-terminal part of PTH to PTH_1R^{ECD} (Step 1a) rigidifies the C-terminal helix as well as residues 6–15 within the N-terminal part of PTH (Step 1b). These conformational changes may expand the small N-terminal helix from residues 6–9 to 6–15. In the slow second step (Step 2), the N-terminal part of PTH is inserted into PTH_1R^{TMD} (Step 2a). Interactions between the N-terminal portion of PTH and PTH_1R^{TMD} and ECL2 residues, promote the formation of a continuous PTH helix (Step 2b). Adapted from Figure 2 in Clark *et al.* (120).

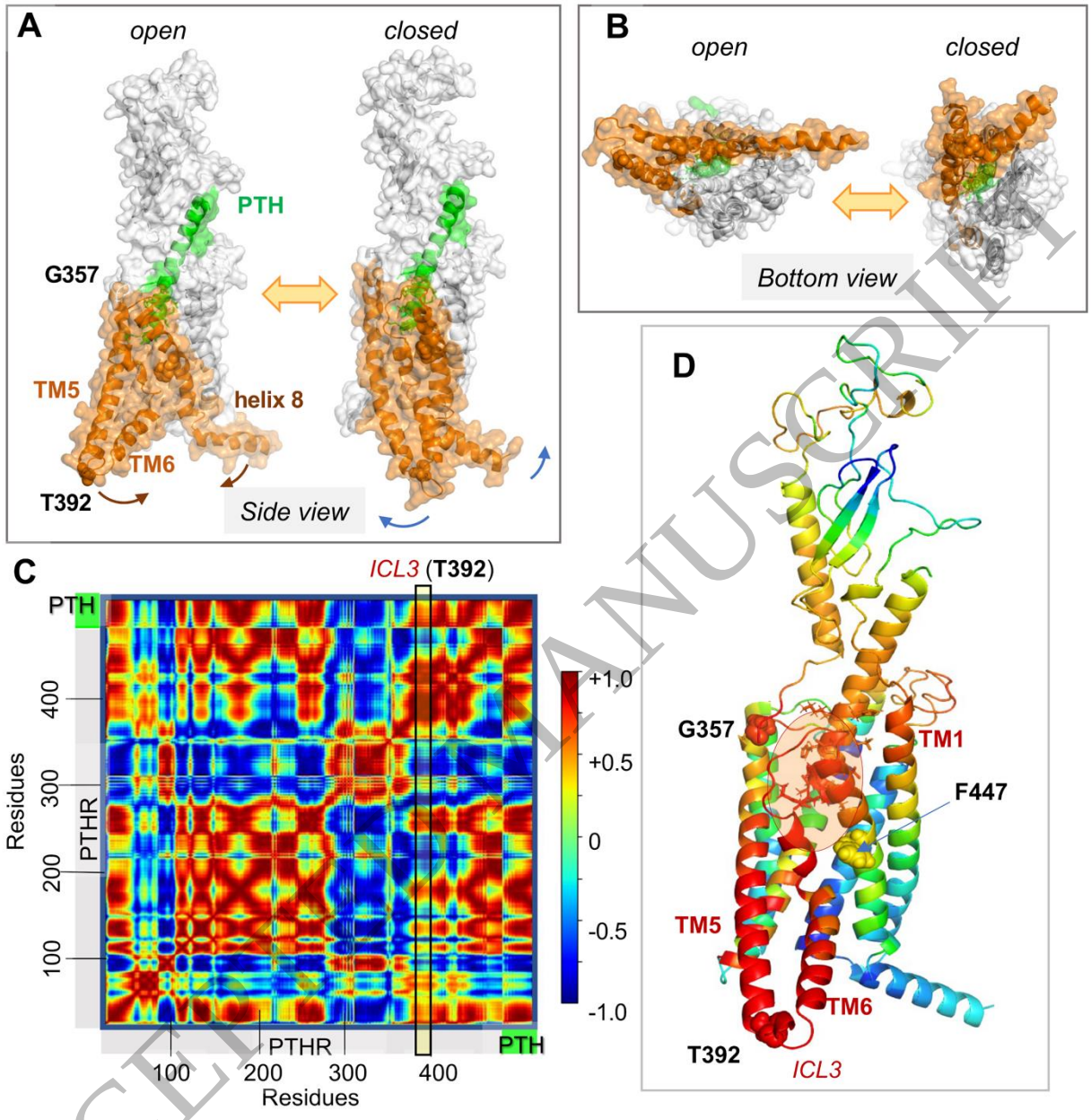

Figure 8. PTH_1R collective dynamics, inter-residue cross-correlations, and allosteric communication. (**A-B**) Collective motions accessible to PTH-bound PTH_1R in the presence of lipid bilayer (not shown). Panels **A** and **B** show the respective side and bottom views of two conformers visited during fluctuations of the complex along ANM mode 14 that cooperatively engages the entire complex. Here, PTH is colored *green*, PTH_1R residues G357-L481, *orange*. Note the large swinging movements at the cytoplasmic ends of TM5-TM6 with respect to helix 8, facilitated by a disruption at TM6. See the corresponding animation in Movie S1. (**C**) Cross-correlation map between residue motions presented in panels **A-B**. The color code refers to the

correlation cosines between the directions of motion of all residue pairs (*scale bar on the right*). *Red* and *blue* regions indicate the regions engaged in strongly correlated (coupled, same direction) and anticorrelated (coupled, opposite direction) movements. (**D**) PTH_1R-PTH complex color-coded by the type and strength of correlations of all residues' movements with the TM5-TM6 cytoplasmic end (derived from the column corresponding to T392 at the ICL3 in panel **C;** see the *vertical box*). *Red* and *blue* residues undergo coupled same and opposite direction fluctuations with respect to T392 (or ICL3). G357, T392, and F447 are displayed in *space-filling*. PTH V1-H14 (enclosed in a semi-transparent *orange ellipse*, residues shown *in sticks*) is strongly correlated with PTHR G357-F447 (*red*) and the N-terminal (extracellularly exposed) part of TM1, and anticorrelated with F447-L481 (*blue*). Adapted from Clark *et al*. (120).

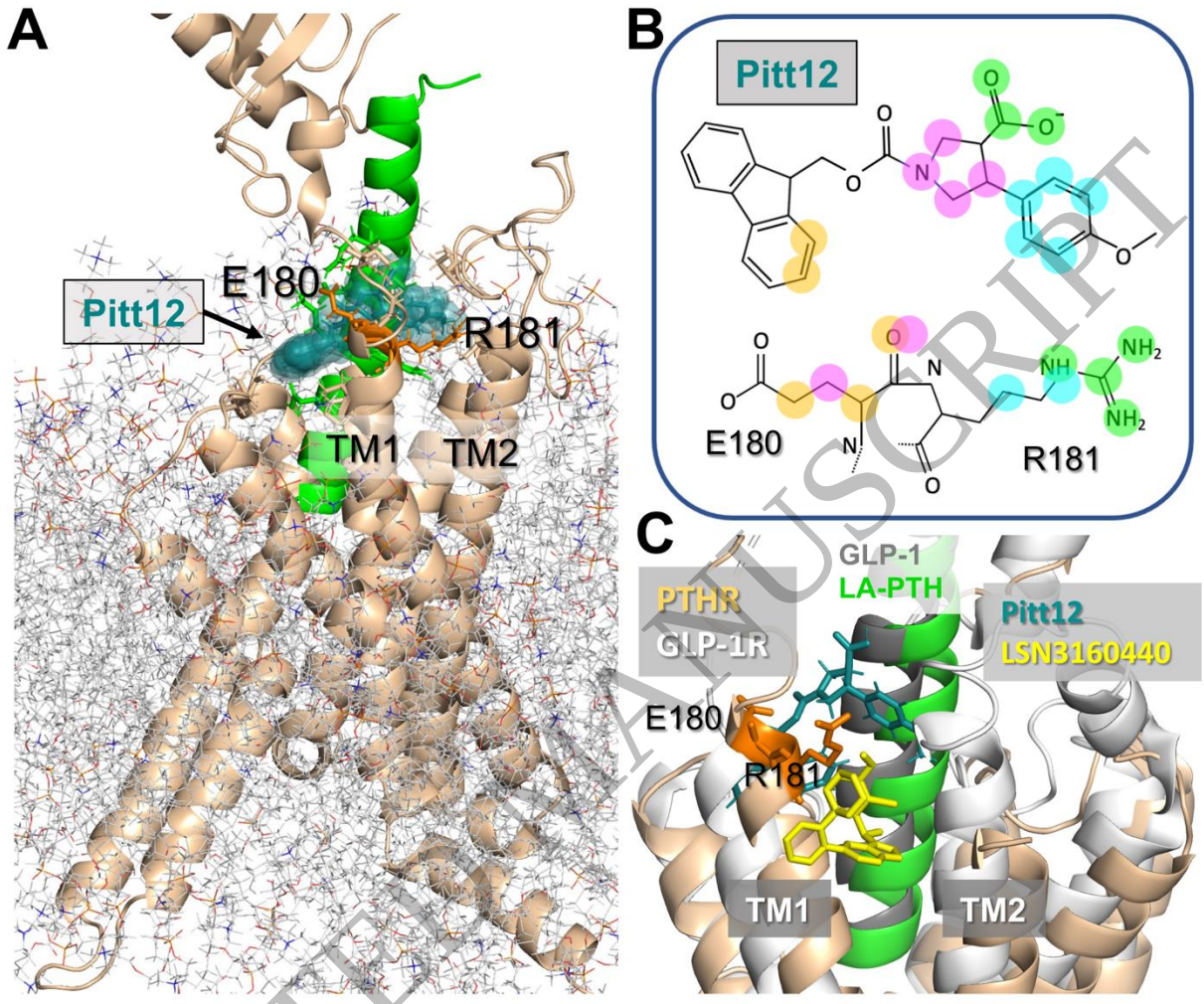

Figure 9. Interaction of a negative allosteric modulator with PTH_1R. (**A**) Results from MD simulations of the binding of an allosteric modulator, named Pitt12, to LA-PTH–bound PTH_1R (PDB 6NBF)(87). The binding pose and structure of Pitt12 were deduced from druggability simulations followed by pharmacophore modeling using Pharmmaker and virtual screening of libraries of small molecules (126). PTH_1R is shown *in wheat ribbon diagram* and LA-PTH in *green*. E180 and R181 (*orange sticks*) were identified as two critical residues that coordinate the small molecule. Pitt12 is shown in teal space-filling. (**B)** 2D representations of Pitt12. Atoms highlighted in *colored spheres* (*at the top*) interact with the E180 and R181 atoms shown by the same color in the diagram *at the bottom*. (**C**) Comparison of the computationally predicted binding pose of Pitt12 onto PTH_1R, and experimentally resolved (127) binding pose of a positive allosteric modulator, LSN3160440, onto GLP-1R (PDB 6VCB) (127). GLP-1R is shown in *light gray*, GLP-1 (structurally aligned against LA-PTH) is in *dark gray*, and LSN3160440 is in *yellow*. Panels A and B are adapted from Sutkeviciute *et al*., (126).

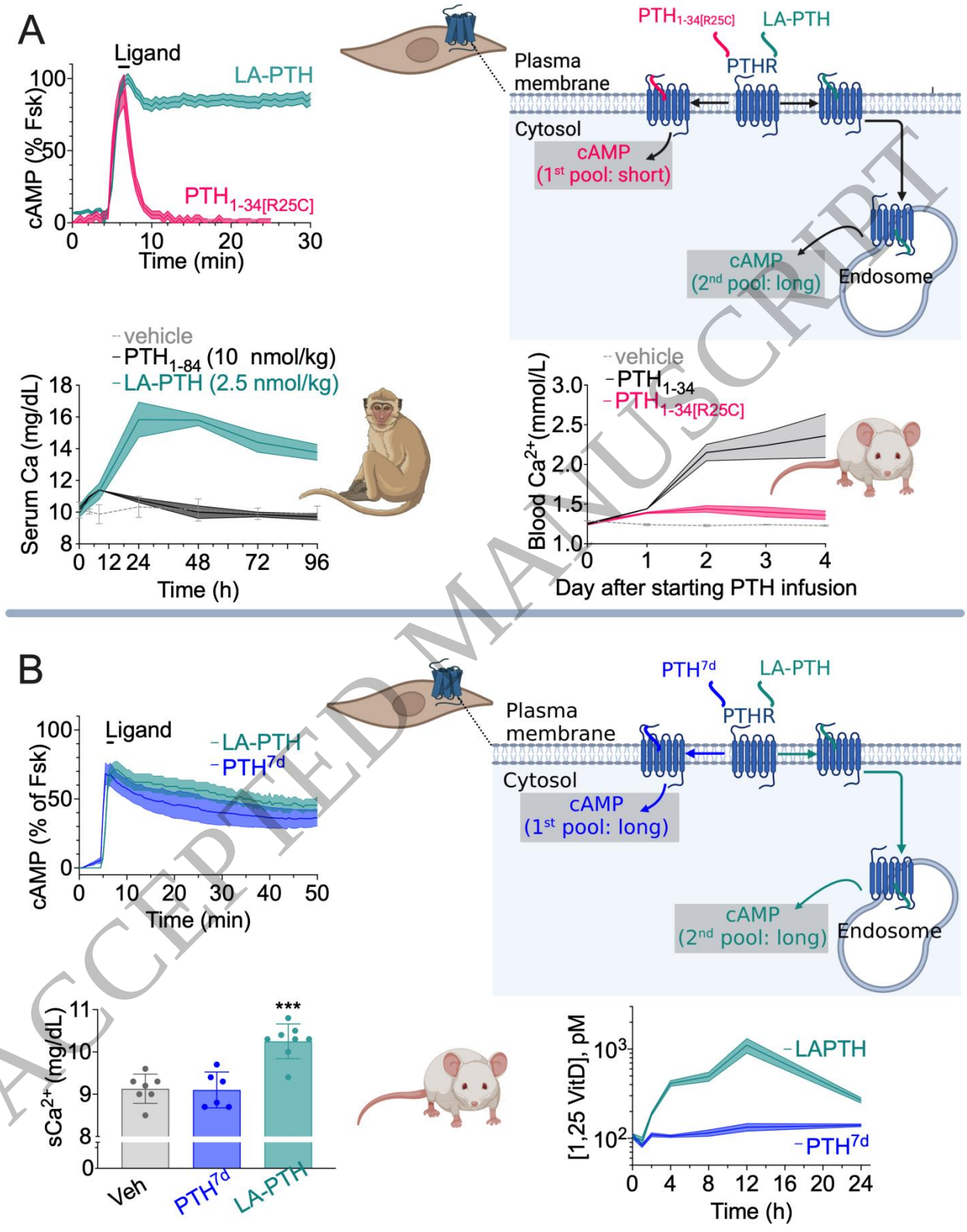

Figure 10. Pharmacological actions of biased PTH ligands in mice. (**A)** Pharmacological actions of LA-PTH and PTH-R25C in cell, mice and monkeys from studies reported in (95,131).

(B) LA-PTH and PTH[7d] are biased PTH agonists inducing a similar sustained cAMP production that originated from distinct cell locations: plasma membrane for PTH[7d] and endosomes for LAPTH. When injected into mice, both ligands induce a similar reduction in serum phosphate ion, however, LAPTH mediates a remarkable increase in serum levels of calcium ion and Vitamin D.

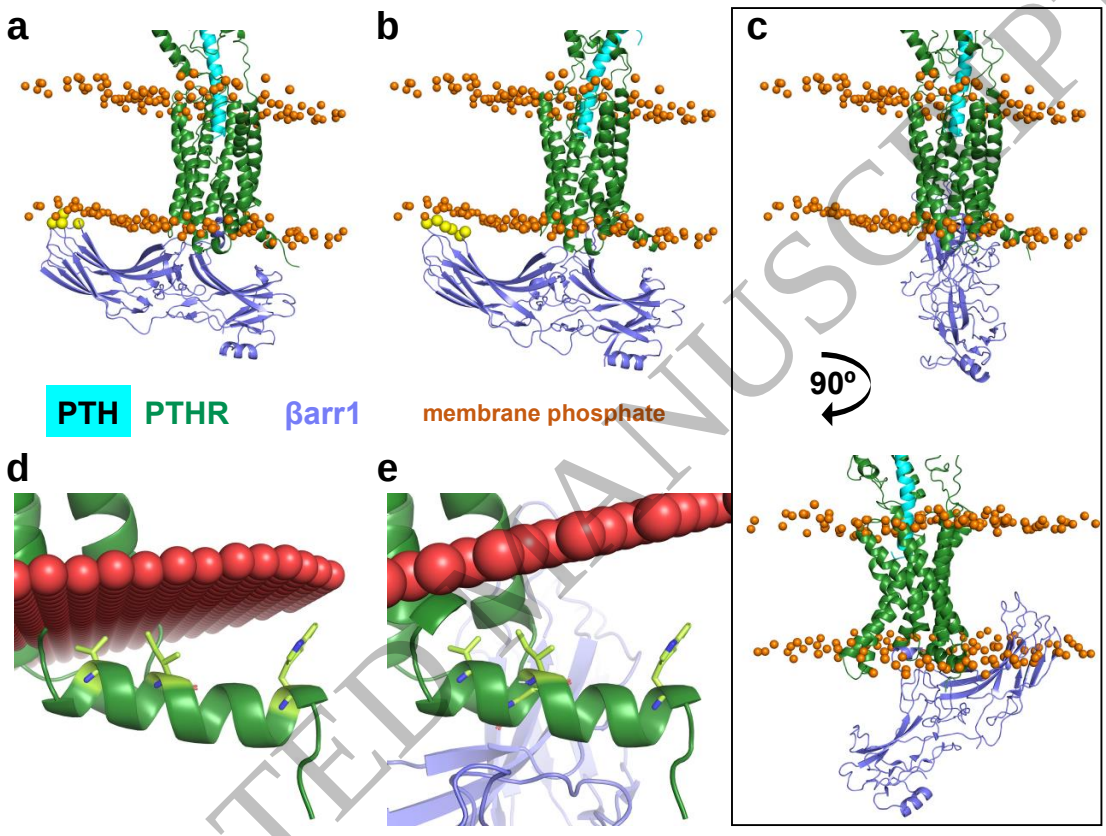

Figure 11. Position of β-arrestin 1 relative to the membrane in PTH_1R–βarr1 models. In all panels, PTH is *cyan*, PTH_1R is *dark green*, and β-arrestin 1 is *slate blue*. The *orange* spheres represent membrane phosphates after 200 ns MD simulation. In A and B, *yellow* spheres are β-arrestin 1 C-edge loop residues that contact the membrane. (**A**) Model 1: PTH_1R–βarr1 model generated using the rhodopsin–arrestin structure (PDB 5W0P) as a template. (**B**) Model 2: PTH_1R–βarr1 model with M2R–βarr1 template structure (PDB 6U1N). (**C-E**) Model 3: PTH_1R–βarr1 model with NTSR1–βarr1 template structure (PDB 6UP7). **C,** *Top*. Model 3 with same orientation as a and b. *Bottom.* Model 3 rotated 90º to highlight significant embedment of β-arr1 C-edge in the membrane. In D and E, PTH_1R alone and Model 3 positioned in membrane (*red*

spheres) by the OPM server. Helix 8 residues from PTH_1R alone interacting with the membrane in panel D are represented as *lime* sticks. Such interactions are eliminated in Model 3.

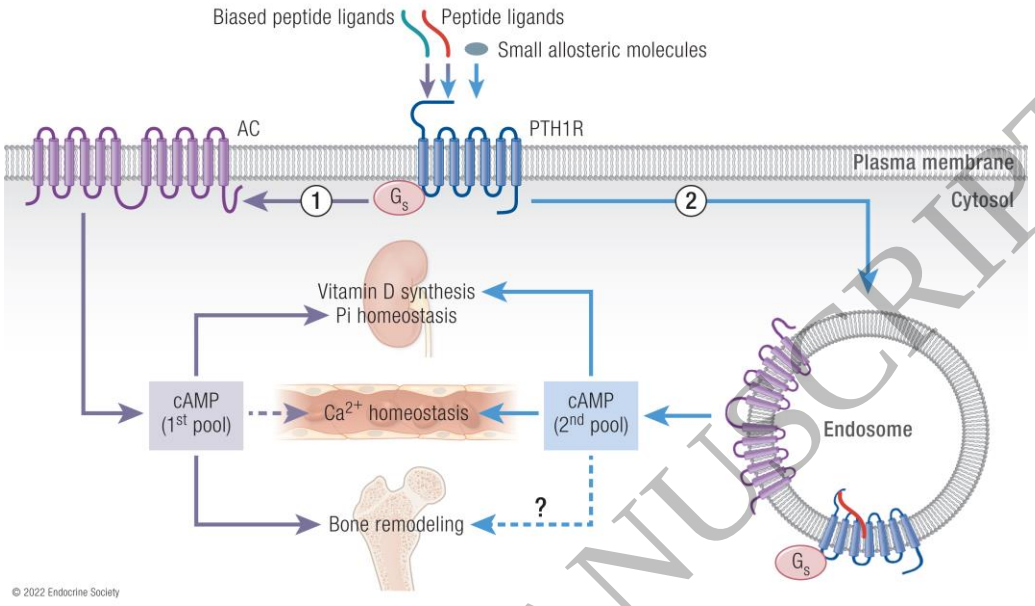

Graphical Abstract

135x81 mm (0.2 x DPI)

List of Essential Points

- Molecular dynamics (MD) simulations linked to anisotropic network model (ANM)-based method address the key question of how to identify druggable allosteric sites in the PTH receptor (PTHR) and small molecules that can execute allosteric modulation of receptor signaling and function.
  - Structure-encoded allosteric coupling between PTHR and PTH residues helps design synthetic PTH analogs with the desired bias to demonstrate that physiological responses to PTH depend on the subcellular location of receptor signaling via cAMP.
- PTHR-generated endosomal cAMP signaling ensures Vitamin D and bone homeostasis whereas the PTHR-generated plasma membrane cAMP maintains phosphate ion homeostasis.